

# SACRA—a method for the estimation of global high-resolution crop calendars from satellite-sensed NDVI

S. Kotsuki<sup>1</sup> and K. Tanaka<sup>2</sup>

[1] Advanced Institute for computational Science, RIKEN, Japan

[2] Disaster Prevention Research Institute, Kyoto University, Japan

Correspondence to: S. Kotsuki ([shunji.kotsuki@riken.jp](mailto:shunji.kotsuki@riken.jp))

## Abstract

To date, many studies have performed numerical estimations of biomass production and agricultural water demand to understand the present and future supply–demand relationship. A crop calendar (CC), which define the date or month when farmers sow and harvest crops, is an essential input for the numerical estimations. This study aims to present a new global data set, the SAteellite-derived CRop calendar for Agricultural simulations (SACRA), and discuss advantages and disadvantages compared to existing census-based and model-derived products. We estimate global CC at a spatial resolution of 5 arc-min using satellite-sensed NDVI data, which corresponds to vegetation vitality and senescence on the land surface. Using the time series of NDVI averaged from three consecutive years (2004–2006), sowing/harvesting dates are estimated for six crops (temperate-wheat, snow-wheat, maize, rice, soybean and cotton). We assume time series of NDVI represent the phenology of one dominant crop and estimate CCs of the dominant crop in each grid. The dominant crops are determined using harvested area based on census-based data. The cultivation period of SACRA is identified from the time series of NDVI, therefore, SACRA considers current effects of human decisions and natural disasters. The difference between the estimated sowing dates and other existing products are less than two months (< 62 days) in most of areas. A major disadvantages of our method is that the mixture of several crops in a grid is not considered in SACRA. The assumption of one dominant crop in each grid is a major source of discrepancy in crop calendars between SACRA and other products. The disadvantages of our approach may be reduced with future improvements based on finer satellite sensors and crop

1 type classification studies to consider several dominant crops in each grid. The comparison of  
2 the CC also demonstrates that identification of wheat type (sowing in spring or autumn) be a  
3 major source of error in global CC estimations.

## 4 5 **1 Introduction**

6 Recent population growth has increased biomass demand significantly, and humans have  
7 expanded cropland globally. Agriculture occupies more than 70% of world water usage and  
8 has a large impact on the water cycle (Rost et al., 2008). Consequently, simulations of  
9 biomass production and agricultural water demand are necessary to understand the present  
10 and future supply–demand relationship. To date, many studies have estimated biomass  
11 accumulation (Fischer et al., 2000; Tan and Shibasaki, 2003; Stehfest et al., 2007) and  
12 agriculture water demand (Döll et al., 2002; Hanasaki et al., 2008; Rockström et al., 2009;  
13 Siebert and Döll, 2009; Pokrel et al., 2011). Those studies estimated biomass production and  
14 agricultural water demand with numerical models using meteorological forcing data and land  
15 surface parameters. A crop calendar (CC) is an essential input to estimate biomass production  
16 and agricultural water demand accurately with those numerical models. CCs define the date or  
17 month when farmers sow and harvest crops. There are three major approaches to develop CC  
18 data sets: census-based; model-based; and Earth observation-based.

19 The first approach, the census-based method, estimates CCs by collecting and integrating  
20 agricultural census data provided by international and national organizations such as the Food  
21 and Agriculture Organization (FAO) and the United States Department of Agriculture  
22 (USDA). The census-based CC products are represented by MIRCA2000 (Portmann et al.,  
23 2010; Monthly Irrigated and Rain-fed Crop Areas around the year 2000) and Sacks et al.  
24 (2010). The census-based products have the advantage of high reliability in regions that have  
25 sufficient census data. However, they also have the disadvantage of low reliability in regions  
26 that have no census data. Additionally, the spatial resolution of census-based products is  
27 limited because of the sampling scheme (Portmann et al., 2010). Because only one CC is  
28 defined per administrative unit for each crop, differences in CCs for the same administrative  
29 unit are not considered.

30 Model-based approaches generate CCs using crop growth models. These models simulate  
31 crop growth based on meteorological forcing data such as temperature, solar radiation, and  
32 soil moisture. In particular, accumulated temperature is widely used to indicate phenological

1 progress. Hanasaki et al. (2008) estimated global CCs for several crops using the soil and  
2 water integrated model (SWIM; Krysnova et al., 2000). Waha et al. (2012) simulated the  
3 sowing dates of major annual crops based on climatic conditions and crop-specific  
4 temperature requirements. The crop growth models have the advantage of accurate crop-  
5 growth simulation in cases of well-calibrated parameters. However, proper calibration is  
6 difficult in areas where observation data are insufficient. Additionally, the crop growth model,  
7 being based on environmental processes, is of limited accuracy with respect to the  
8 identification of sowing dates, because the sowing date is heavily affected by human  
9 decisions.

10 Finally, Earth observation-based studies estimate the CC using time series from satellite  
11 observations. Time series of vegetation indices (VIs) correspond well to vegetation vitality  
12 and senescence on the land surface. In this context, satellite-derived VIs have been widely  
13 used to classify crop type and to monitor crop growth at the regional scale (Mingwei et al.,  
14 2008; Sakamoto et al., 2005; Sakamoto et al., 2010; Wardlow and Egbert, 2008; Wardlow et  
15 al, 2007). An advantage of satellite-derived data is its spatial resolution (less than 1 km).  
16 However, few studies have estimated global CCs with satellite-derived data. Yorozu et al.  
17 (2005) estimated a global CC using the normalized difference vegetation index (NDVI), but  
18 they did not compare their results to other global CC data sets.

19 In this paper, we present a new global data set, the SATellite-derived CRop calendar for  
20 Agricultural simulations (SACRA). Using satellite-sensed NDVI data, we estimate the global  
21 CC at a spatial resolution of 5 arc-min (~ 9.2 km at the equator). This study aims to develop a  
22 high-resolution and highly-accurate CC product by combining satellite-derived NDVI with a  
23 census-based product. We also aim to discuss the advantages and disadvantages of our  
24 satellite-derived CC, compared to existing census-based and model-derived products. The  
25 products are available for download at [http://data-](http://data-assimilation.jp/opendata/sacra/sacra_des.html)  
26 [assimilation.jp/opendata/sacra/sacra\\_des.html](http://data-assimilation.jp/opendata/sacra/sacra_des.html)

## 27 **2 Materials and Methods**

28 This section describes the methods applied to produce the SACRA according to a defined  
29 data processing scheme (Fig. 1). The SACRA is produced from four different data sets: time  
30 series of NDVI; land cover data; reanalysis temperature data; and census-based agricultural  
31 data (Table 1). This study estimates the CC for six crops (temperate-wheat, snow-wheat, rice,  
32 maize, soybean, and cotton) that are widely cultivated around the world (Table 2a). We treat

1 temperate-wheat and snow-wheat separately because our method is unsuitable for estimating  
2 sowing date in grid areas where the surface is covered by snow during the cultivating period  
3 (e.g., Russia and North China; see Subsection 2.3 for details).

4 The following subsections describe identification of the dominant crop and census-based  
5 CC (Subsection 2.1), vegetation indices (Subsection 2.2), estimation of global crop calendar  
6 (first estimation; Subsection 2.3) and the SACRA data sets (Subsection 2.4).

## 7 **2.1 Dominant crop and census-based sowing/harvesting data**

8 Firstly, we identify the dominant crop at a spatial resolution of 5 arc-min using  
9 MIRCA2000. The grid of the SACRA is set to that of MIRCA2000. Portmann et al. (2010)  
10 compiled irrigated and rain-fed areas of 26 crop types at a spatial resolution of 5 arc-min (cf.  
11 Table 4 in Portmann et al., 2010). In other words, we can obtain 52 classes of crop areas at  
12 each grid (i.e., both irrigated and rain-fed areas of 26 crop types). Their crop calendars in  
13 major and second cultivation seasons are also defined in MIRCA2000. Since our method  
14 cannot consider the mixture of several crops in a grid (see Subsection 2.2.2 for details), we  
15 consider only one dominant crop in each grid. We define the dominant crop in the major  
16 cultivation season as that which has the maximal harvested area in the grid, out of 52 possible  
17 crops (considering rain-fed and irrigated areas separately; cf. Appendix I in Portmann, 2011).  
18 If more than two crops have identical harvested areas, the early order of the crops is chosen to  
19 be the dominant crop (e.g., for irrigated wheat in India Uttar Pradesh with two identical areas  
20 with different cropping periods; cf. Table I-211 of Appendix I in Portmann, 2011). The  
21 dominant crop in the second cultivation season is determined from those crops whose  
22 cultivation periods do not overlap more than three months with that of the dominant crop in  
23 the major cultivation season.

24 Secondly, we obtain the sowing and harvesting months of the dominant crop in both major  
25 and second cultivation seasons, using MIRCA2000. At each grid, we use the sowing and  
26 harvesting months. The census-based sowing and harvesting months are used to calibrate crop  
27 calendar parameters in Subsection 2.3.

28 Finally, we classify temperate-wheat and snow-wheat (originally classified as “wheat” in  
29 MIRCA2000) using reanalysis temperature data (Table 2). Again, our method is unsuitable  
30 for the estimation of sowing date for grids where the surface is covered by snow during  
31 cultivation. If the minimum monthly-averaged temperature during the cultivating period is

1 below 5.0 °C, the wheat is categorized as snow-wheat. In this categorisation, we use  
2 MIRCA2000-derived cultivating periods (from sowing month to harvesting month) and  
3 reanalysis temperature (Hirabayashi et al., 2008). Hirabayashi et al. (2008) compiled 3-hourly  
4 surface temperature data by statistical methods, the parameters of which had been obtained  
5 from available surface observations. Here, we simply use the reanalysed temperature of the  
6 nearest 30 arc-min grid from MIRCA2000's 5 arc-min grids.

7 The resulting global distribution of dominant crops in SACRA in the major cultivation  
8 season is shown in Fig. 2a. The minimum monthly-averaged temperature during the  
9 cultivation period of the dominant crop is shown in Fig. 2b. Regions showing the minimum  
10 monthly-averaged temperatures below 5.0 °C in Fig. 2b are categorized as snow-wheat  
11 (purple) or other crops (grey) in Fig. 2a. The categories of temperate-wheat and snow-wheat  
12 classify whether or not surface is covered by snow during cultivation. Note that the  
13 classification of temperate-wheat and snow-wheat is independent of the classification of  
14 spring-wheat and winter-wheat. The classification of spring-wheat and winter-wheat depends  
15 on the sowing season (spring or autumn).

## 16 **2.2 Vegetation index**

### 17 **2.2.1 VEGETATION/SPOT NDVI data**

18 Vegetation indices are simple, graphic indicators to assess whether the targeting area  
19 contains live, green vegetation or not. In this study, we use NDVI defined by the following:

$$20 \quad NDVI = \frac{NIR - VIS}{NIR + VIS} \quad (1)$$

21 where *VIS* and *NIR* indicate the spectral reflectance in the visible and near-infrared bands. The  
22 formula is based on the fact that chlorophyll absorbs *VIS*, whereas the mesophyll leaf  
23 structure scatters *NIR* (Pettorelli et al., 2005). NDVI correlates with the accumulation and  
24 decomposition of leaf cell tissue. Therefore, we are able to detect crop growth with the time  
25 series of NDVI over the cropland. The time series of satellite-sensed NDVI at a double-  
26 cropping pixel in China is shown in Fig. 3a. As shown in Fig. 3a, peak dates can be clearly  
27 identified from the time series of NDVI. In this study, we use a 10-day composite NDVI  
28 provided by VEGETATION/SPOT (Maisongrande et al., 2004). To reduce the effect of  
29 clouds, the best index slope extraction (BISE) method (Viovy et al., 1992) is applied to the  
30 time series of NDVI (Fig. 3a). To estimate the CC with the smooth time series of NDVI, we

1 use averaged NDVI over three years (2004–2006). Hereafter, this averaged NDVI is indicated  
 2 by SPOT-NDVI in this manuscript. The time series of NDVI has inter-annual variability as  
 3 shown in Fig. 3b.

#### 4 **2.2.2 Aggregation of NDVI**

5 Two NDVI data sets (NDVI-Pure and NDVI-Crop; 5 arc-min resolution) are aggregated  
 6 from original SPOT-NDVI (1-km resolution) using two land-cover data sets: Global Land  
 7 Cover Characterization, version 2.0 (GLCC; Loveland et al., 2000) and Ecoclimap, version  
 8 2.0 (Faroux et al., 2013). The GLCC and Ecoclimap data are provided by the U.S. Geological  
 9 Survey and Meteo France, respectively. Schematic imagery of the aggregated NDVI-Pure and  
 10 NDVI-Crop data is shown in Fig. 4. The NDVI-Pure and NDVI-Crop data are aggregated by  
 11 averaging 1-km NDVI pixels where both GLCC and Ecoclimap agree on the cropland (i.e., at  
 12 a higher level confidence; Fig. 4a). However, it is possible for there to be no pixel where both  
 13 GLCC and Ecoclimap agree on the cropland. In this case, only the NDVI-Crop is aggregated  
 14 by averaging the pixels where the GLCC and Ecoclimap disagree, but where one of them  
 15 agrees on cropland (i.e., a lower level confidence; Fig. 4b). The NDVI-Pure is undefined in  
 16 the latter case. The NDVI-Pure, containing only higher confidence grids, is used to identify  
 17 the two CC parameters (Subsection 2.3). The NDVI-Crop is used to produce the global CC in  
 18 Subsection 2.4. The two aggregations (spatial and temporal) aim to obtain a smoother time  
 19 series of the NDVI by removing the phenology of non-dominant and voluntary crops.

#### 20 **2.2.3 Normalization of NDVI**

21 Absolute peak values of NDVI differ depending on climate conditions and density of  
 22 crops. Therefore, we normalize NDVI data to consider variety over a wide range of  
 23 environmental conditions at the global scale. First, we identify cropping intensity using the  
 24 time series of the NDVI. We define the peak of the NDVI ( $NDVI_{pk}$ ) and the date of the peak  
 25 ( $t_{pk}$ ) if the time series of the NDVI satisfy Equations (2) and (3):

$$26 \quad NDVI(i) \leq NDVI(t_{pk}) \quad (i = t_{pk} - 1, t_{pk} - 2, \dots, t_{pk} - 6) \quad (2)$$

$$27 \quad NDVI(i) \leq NDVI(t_{pk}) \quad (i = t_{pk} + 1, t_{pk} + 2, \dots, t_{pk} + 4) \quad (3)$$

28 where the boundary is cyclic (i.e.,  $NDVI_0 = NDVI_{36}$ , and  $NDVI_l = NDVI_{37}$ ) since we have 36  
 29 NDVI data per year from 10-day composite data of the SPOT-NDVI. We assume an  
 30 increase/decrease in the NDVI before/after the peak of the NDVI, as shown in Eqs. (2) and

1 (3). The cropping intensity is equal to the number of peaks of the NDVI, up to three times per  
2 year. Second, we detect the lowest NDVI between peaks ( $NDVI_{btm}$ ). Finally, NDVI data is  
3 normalized using the following equations:

$$4 \quad nNDVI(t) = \frac{NDVI(t) - NDVI_{bas}}{NDVI_{pk} - NDVI_{bas}} \quad (4)$$

$$5 \quad NDVI_{bas} = \max(NDVI_{btm}, NDVI_{snow}) \quad (5)$$

6 where nNDVI represents normalized NDVI. Subscripts *btm*, *bas*, and *snow* denote bottom,  
7 base and snow, respectively. The  $NDVI_{snow}$  is a parameter to avoid remnant irregular NDVI  
8 mainly caused by snow cover reflection. The  $NDVI_{snow}$  is set at 0.20, which corresponds to 40  
9 % of the snow cover over the land surface (Dye and Tucker, 2003). Fig. 3c shows a schematic  
10 image of the normalization of NDVI at the double-cropping pixel in China. As shown in Fig.  
11 3c, the  $NDVI_{bas}$  can be different for each peak. We do not need to avoid the negative nNDVI  
12 in this normalization process. The normalization is applied for both the NDVI-Pure and the  
13 NDVI-Crop.

14 The detected cropping intensity with the NDVI-Crop is compared with a climate-based  
15 estimation (Zabel et al., 2014). Zabel et al. (2014) estimated potential cropping intensity (i.e.,  
16 maximal cropping intensity) suitability for current climate conditions (1981–2010) for 16  
17 crop types (Table 2b). Detected and estimated cropping intensities are shown in Figs. 5a and  
18 5b. Since Zabel et al. (2014) estimated cropping intensities for 16 crops, we illustrate the  
19 cropping intensity of the dominant crop in the major cultivation season in SACRA. The  
20 location of six administrative units are emphasized with boxes (A–F) in Figs. 5a and 5b,  
21 where our estimations are different from those of Zabel et al. (2014).

22 Table 3 shows a comparison of estimated cropping intensity in this study and that of Zabel  
23 et al. (2014) for the six administrative units (six boxes A–F in Figs. 5a and 5b). For the  
24 comparison, simplified cropping intensity for irrigated (IRC) and rain-fed (RFC) crop classes  
25 from MIRCA2000 are also described. Here, simplified cropping intensities are defined as  
26 “annual harvested area” divided by “maximum monthly cropped area”, which are defined for  
27 both irrigated and rain-fed classes of 26 crop types in MIRCA2000. The averaged cropping  
28 intensities over the administrative units are shown in the table. We illustrate the time series of  
29 the NDVI-Crop in the six administrative units in Fig. 6 to investigate the difference in  
30 cropping intensity. The time series of the NDVI-Crop, averaged over the administrative units,

1 are shown in Fig. 6 for 2004, 2005, 2006, and averaged from 2004 to 2006 (red, blue,  
2 magenta, and green lines in Fig. 6).

3 In Brazil Rio Grande do Sul (box A), and U. S. Mississippi (box F), the average cropping  
4 intensity in this study is smaller than in Zabel et al. (2014). On the other hand, our estimations  
5 are close to the simplified cropping intensity by MIRCA2000. Zabel et al. (2014) estimated  
6 potential cropping intensity, which provides a reason for the overestimation of cropping  
7 intensity compared to our study. A mixture of bimodal and nearly constant NDVI-Crop (black  
8 lines) is shown in Brazil Rio Grande do Sul (Fig. 6A). The nearly constant NDVI is  
9 characteristic of a tropical forest. The NDVI-Crop data may not represent the phenology of  
10 the cropland in some grids because of uncertainty of the land cover data and insufficient  
11 spatial resolution (see Subsection 3.3 for further discussion).

12 In China Henan (box B), India Uttar Pradesh (box D), and Kenya (box E), the average  
13 cropping intensity in this study is larger than in Zabel et al. (2014) and MIRCA2000, with the  
14 only exception being irrigated crop in MIRCA2000 in India Uttar Pradesh. In India Uttar  
15 Pradesh, harvested area of irrigated crops is larger than that of rain-fed crops (cf. Table I-211  
16 in Portmann 2011), suggesting our estimation of cropping intensity correspond to the irrigated  
17 crop. We see clear trimodal and bimodal NDVI-Crop (green lines) in In China Henan, and  
18 Kenya (Fig. 6B and 6E). Again, Fig. 5b shows the average cropping intensity for the  
19 dominant crop in the major cultivation season, according to Zabel et al. (2014). Generally,  
20 farmers do not conduct multiple cropping with only wheat. Zabel et al. (2014) reported  
21 multiple-cropping intensities for other crops in two administrative units. The other possibility  
22 is that overestimations of cropping intensity derive from mixture of phenology from different  
23 crops or vegetation in France (box C). On the other hand, Zabel et al. (2014) and  
24 MIRCA2000 may underestimate cropping intensity in Kenya, where a clear bimodal NDVI-  
25 Crop (green line) is detected in Fig. 6E. It is also possible the bimodal NDVI-Crop can be  
26 derived from mixture of phenology from different crops.

### 27 **2.3 First estimation of global crop calendar**

28 This study estimates sowing and harvesting dates ( $t_{sw}$  and  $t_{hv}$ ) using two CC parameters  
29 ( $nNDVI_{sw}$  and  $nNDVI_{hv}$ ) and a time series of nNDVI data. The sowing and harvesting dates  
30 are determined by the following:



$$1 \quad t = \begin{pmatrix} t_{sw} \\ t_{hv} \end{pmatrix} \text{ when } \begin{pmatrix} t \leq t_{pk} & \text{and} & nNDVI(t) \geq nNDVI_{sw} \\ t \geq t_{pk} & \text{and} & nNDVI(t) \leq nNDVI_{hv} \end{pmatrix} \quad (6)$$

2 where subscripts  $sw$ , and  $hv$  denote sowing, and harvest, respectively. Figs. 7a and 7b show  
3 schematics of identification of sowing and harvesting dates for temperate crops (temperate-  
4 wheat, rice, maize, soybean, and cotton) and snow-wheat. In the multiple cropping grids,  
5 sowing and harvesting dates are also determined for each cropping season (except for sowing  
6 date of snow-wheat). Our method is unsuitable for the estimation of sowing dates of snow-  
7 wheat because we assume an increase in NDVI from sowing date to peak in Eq. (6).  
8 However, NDVI decreases if the surface is covered by snow (Fig. 7b). Therefore, in this  
9 process, we determine both sowing and harvesting dates for temperate crops, and only  
10 harvesting date for snow-wheat. The two CC parameters, used for the determination of  
11 sowing and harvest dates, are defined for each crop type with the exception of the  $nNDVI_{sw}$  of  
12 snow-wheat. We calibrated the two CC parameters ( $nNDVI_{sw}$  and  $nNDVI_{hv}$ ) for each crop type  
13 as described in the following paragraph.

14 To remove the noise of the time series of NDVI data as much as possible, we use limited  
15 grids (hereafter, calibration grids) to estimate the two CC parameters. The calibration grids  
16 satisfy the following conditions: 1) single cropping defined by cropping intensity; 2)  
17 dominant crop occupying more than 25 % of the total cropland area (using land-cover fraction  
18 data from 26 crop types in MIRCA2000); 3) up to five grids from the same administrative  
19 unit of MIRCA2000; 4)  $NDVI_{pk}$  is larger than  $NDVI_{snow}$ ; and 5) containing NDVI-Pure (i.e.,  
20 using only higher-level confident grids). Once the parameters  $nNDVI_{pl}$  and  $nNDVI_{hv}$  are  
21 determined, sowing and harvesting dates can be determined using Eq. (6). The values of the  
22 two CC parameters  $nNDVI_{pl}$  and  $nNDVI_{hv}$  are calibrated for each crop to minimize the errors  
23 over calibration grids between determined sowing/harvesting dates and MIRCA2000 (see  
24 Appendix A for details). Table 4 shows the number of calibration grids, the calibrated two  
25 CC parameters and averaged errors in sowing/harvesting dates for six crop types.

## 26 **2.4 SACRA data sets**

27 The global sowing and harvesting dates are determined by Eq. (6) using time series of the  
28 nNDVI-Crop) and two CC parameters (first estimation in Fig 1; except for sowing date of  
29 snow-wheat). Our method detects the cultivation season using time series of the satellite-  
30 sensed NDVI. However, our algorithm carries the possibility of overestimating or

1 underestimating cultivation periods. The cultivation period (from sowing date to harvesting  
2 date) in our scheme is largely affected by the shape of the NDVI (i.e., kurtosis of the NDVI  
3 curve). Therefore, our method can result unrealistic cultivation periods in some grids (e.g.,  
4 less than 60 days) if NDVI-Crop does not represent the phenology of the dominant crops due  
5 to mixture of phenology from other crops and vegetation. Therefore, we adjust the length of  
6 the cultivation period to be equal to MIRCA2000 to avoid the unrealistic cultivation periods.  
7 For the temperate crops, sowing and harvesting dates are moved (advanced or postponed) to  
8 adjust the cultivation period to MIRCA2000. In this treatment, the ratio of  $t_{pk}-t_{sw}$  to  $t_{hv}-t_{pk}$  is  
9 preserved as the ratio of  $t_{pk}-t_{sw-adj}$  to  $t_{hv-adj}-t_{pk}$ , (Fig. 8a), where  $t_{sw}$  (or  $t_{hv}$ ) and  $t_{sw-adj}$  (or  $t_{hv-adj}$ )  
10 denote sowing (or harvesting) dates for the first estimation and after the adjustment,  
11 respectively. For snow-wheat, the harvesting date is fixed (i.e.,  $t_{hv}=t_{hv-adj}$ ). The sowing date is  
12 determined by the cultivation period of MIRCA2000 and the harvesting date of the first  
13 estimation (Fig. 8b). Here, we use the cultivation period in MIRCA2000 from the 15th of the  
14 sowing month to the 15th of the harvesting month. For multiple-cropping grids, the  
15 corresponding cultivation season in MIRCA2000 (i.e., major or second cultivation seasons)  
16 from each cropping is determined by the following:

$$17 \quad \begin{pmatrix} major & season \\ second & season \end{pmatrix} \text{ when } \begin{pmatrix} Mon_{sw(major),1st} \leq t_{pk} < Mon_{sw(second),1st} \\ Mon_{sw(second),1st} \leq t_{pk} < Mon_{sw(major),1st} \end{pmatrix} \quad (7)$$

18 where  $Mon_{sw,1st}$  denotes the 1st of the sowing month in MIRCA2000. Subscripts *major* and  
19 *second* denote major and second cultivation seasons, respectively. Here, we consider the  
20 cyclic boundary of the calendar. We apply the cultivation period of the major cultivation  
21 season in grids where no dominant crop in the second cultivation season is defined. The  
22 adjusted sowing and harvesting dates are referred to as SACRA and discussed in the next  
23 section.

### 24 **3 Results and discussion**

25 This section provides validation and discussion regarding the produced SACRA data set.  
26 However, true validation is hard to achieve in global studies. Therefore, we compare the  
27 estimated CC with other CC data produced using other estimations, either census-based or  
28 model-based.

### 1 3.1 Comparison with census-based and model-based approaches

2 We compare the SACRA with two CC data sets: MIRCA 2000, and Waha et al. (2012;  
3 hereafter W12). We selected MIRCA2000 and W12 arbitrarily as representing census-based  
4 and model-based CC data, respectively. Waha et al. (2012) simulated the sowing dates of  
5 major annual crops from 1900 to 2003 at a spatial resolution of 0.5 degrees. We use the  
6 averaged sowing dates (2000–2003) of four crops (wheat, rice, maize and soybean) from W12  
7 for comparison. Waha et al. (2012) assigned 1st January as the sowing date, as it is as good as  
8 any other day for sowing in a favourable all-year climate. Therefore, averaged sowing dates  
9 are computed, excluding grids assigning 1st January for sowing date. Note that the sowing  
10 date of cotton was not estimated in W12. The averaged sowing date over years is computed  
11 by the following:

$$12 \quad \eta_{year,sw} = F \left( DOY_{year,sw} \right) = \frac{DOY_{year,sw}}{\text{Days of the year}} \cdot 2\pi \quad (8)$$

$$13 \quad DOY_{ave,sw} = F^{-1} \left\{ \arg \left( \text{average} \left( \cos(\eta_{year,sw}) \right) + i \cdot \text{average} \left( \sin(\eta_{year,sw}) \right) \right) \right\} \quad (9)$$

14 where, DOY,  $\eta$ , arg, and  $i$  denote day of year, angle of the DOY (rad), argument, and  
15 imaginary unit, respectively, and subscript *ave* denotes average.  $F$  and  $F^{-1}$  define functions to  
16 compute  $\eta$  from DOY, and DOY from  $\eta$ , respectively. Eqs. (8) and (9) are used to compute  
17 the averaged sowing date considering the cyclic boundary of the calendar.

18 The spatial distributions of the sowing dates for the dominant crops in the major cultivation  
19 season for SACRA, MIRCA2000 and W12 are shown in Fig. 9. The sowing dates are  
20 illustrated in grids where the dominant crop of SACRA in the major cultivation season is  
21 temperate-wheat, snow-wheat, maize, rice, soybean or cotton. If multiple sowing exists in the  
22 SACRA dates for the major cultivation season, we illustrate the sowing dates derived from  
23 the largest  $NDVI_{pk}$  among the sowing dates. For MIRCA2000, we illustrate the 15th of the  
24 sowing month. Although three different sets of data are produced from the different  
25 approaches (Earth observation-based, census-based, and model-based), they have similar  
26 spatial patterns (Figs. 9a-1, 9b-1, and 9c-1). Their sowing dates generally represent spring in  
27 their grids. Figs. 9a-2, 9b-2, and 9c-2 show the sowing dates in South Asia, selected  
28 arbitrarily to highlight the higher spatial variability in SACRA. Since SACRA uses high-  
29 resolution satellite data, it reflects a variety of sowing dates in the same administrative unit, as  
30 shown in Fig. 9a-2 (e.g., Thailand, Vietnam, and Laos). W12 also resulted in a variety of

1 sowing dates for Vietnam (9c-2) due to the estimation being based on climatic data. The  
2 detection of variability in the CC within an administrative unit is an advantage of Earth-  
3 observation-based and model-based approaches compared to census-based methods. On the  
4 other hand, SACRA carries the disadvantage of undetection of a crop calendar in grids where  
5 the NDVI-Crop is not defined (boxes in Figs. 9a-2, 9b-2, and 9c-2).

6 While SACRA can detect the variability of the CC within administrative units, it is  
7 difficult to demonstrate whether the variability is correct around the globe without knowledge  
8 of the local CC information. Therefore, the following subsection discusses the differences in  
9 the CCs among the three products, with sowing dates. We compare the sowing dates of the  
10 three products averaged over administrative units defined in MIRCA2000.

### 11 **3.2 Comparison of averaged CC over MIRCA2000 administrative units**

12 To investigate the characteristics of the three approaches, we compare the averaged sowing  
13 dates over administrative units. The averaged sowing dates of the dominant crop in the major  
14 cultivation season are computed by three products (SACRA, MIRCA2000, and W12) using  
15 Eqs. (8) and (9), averaging not over years but over administrative units. We assign the 15th of  
16 the sowing month for MIRCA2000. The sowing dates of temperate- and snow-wheat in  
17 SACRA are compared with the sowing dates of “wheat” in MIRCA2000 and W12. Here, only  
18 single cropping grids are used to compute the averaged sowing date for SACRA. We suppose  
19 that  $NDVI_{bas}$  represents condition with few vegetation in winter (or dry) season. In the  
20 multiple cropping grids, the  $NDVI_{bas}$  in summer (or wet) season can be higher than other  
21 seasons due to mixture of phenology from other crops and vegetation (e.g.,  $NDVI_{bas}$  in June is  
22 higher than that in December in Fig. 3c). Therefore, accuracy of CCs in multiple cropping  
23 grids may be lower than that in single cropping grids.

24 The differences in the sowing dates of the dominant crop are shown in Fig. 10. The  
25 administrative units are illustrated if their dominant crop in the major cultivation season is  
26 temperate-wheat, snow-wheat, maize, rice, soybean or cotton. The difference for each specific  
27 crop type is shown in Fig. A3. The difference between the two data sets is less than two  
28 months ( $< 62$  days; yellow- or green-coloured units) in most of the administrative units in  
29 Figs. 10a and 10b. Fig. A3 shows that wheat contains the largest number of units with a large  
30 difference in sowing dates ( $> 93$  days; red- or blue-coloured units). We observe a later  
31 signalling trend in sowing dates in SACRA than in W12 (Fig. 10b; green- or blue-coloured

1 units). The direction of the later signalling trend is dominant in wheat, maize, rice and  
2 soybean (Figs. A3-a2, A3-b2, A3-c2, and A3-d2).

3 Table 5 compares the sowing dates of the three products in 16 administrative units that fall  
4 into the category of disagreement (more than 150 days) between SACRA and MIRCA2000 or  
5 SACRA and W12. We present the cultivation seasons (from sowing to harvesting dates) in 16  
6 administrative units in Fig. A4 to understand the discrepancies in the CCs of the three  
7 products. To interpret the disagreements in Table 5 and Fig. A4, we use Fig. 11, which shows  
8 the time series of the NDVI-Crop, average NDVI-Crop, average NDVI-Forest, and average  
9 temperature data. Here, average means the average over administrative units. NDVI-Forest is  
10 produced by following NDVI-Crop production, but with forest pixels using GLCC and  
11 Ecoclimap land cover data. Namely, NDVI-Forest is aggregated by averaging the pixels  
12 where the GLCC or Ecoclimap agree on forest.

13 We observe disagreements in 12 administrative units where the dominant crops in the  
14 major cultivation season are temperate- or snow-wheat, shown in Table 5. Cultivated wheat in  
15 the world can be classified into two types depending on the sowing season. The FAO (2002)  
16 notes the following: 1) the first type of wheat is planted in the autumn to germinate and  
17 develop into young plants that remain in the vegetative phase during the winter and resume  
18 growth in the early spring; 2) the second type of wheat is usually planted in the spring and  
19 matures in late summer but can be sown in autumn in countries that experience mild winters,  
20 such as in South Asia, North Africa, the Middle East and at lower latitudes.

21 In Azerbaijan (code 8), and Kazakhstan (code 225), large differences ( $> 150$  days) are  
22 observed between SACRA and W12, while the differences between SACRA and  
23 MIRCA2000 are  $< 50$  days. In Australia Queensland (code 36), China Gansu (code 102),  
24 China Ningxia (code 117), and India Himachal Pradesh (code 192), a large difference is  
25 observed between SACRA and MIRCA2000. In the above six administrative units, the  
26 assumed wheat type may be incorrectly identified in MIRCA2000 and W12. On the other  
27 hand, SACRA's sowing dates differ from both MIRCA2000 and W12 for Beijing (code 99),  
28 Hebei (code 107), Henan (code 109), Shaanxi (code 119), Shandong (code 120), and Shanxi  
29 (code 122) in China. In these six administrative units, SACRA has possibly detected incorrect  
30 signals of NDVI (e.g., signals of forest or other crops). As shown in Fig. A3, wheat is related  
31 to the largest number of units with disagreements in sowing dates. Disagreements in sowing

1 dates are also observed between MIRCA2000 and W12. The identification of wheat type  
2 (sowing in spring or autumn) may be a major source of error in global CC estimations.

3 In Bhutan (code 49), India Sikkim (code 207), and Uruguay (code 394), clear unimodal  
4 NDVI-Crops are not observed in Fig. 11. The accuracy of SACRA is affected by the accuracy  
5 of the land cover data sets. It is known that the 1-km land cover data sets contain uncertainties  
6 (Herold et al., 2008; Nakaegawa, 2011). For example, forests may be classified as croplands  
7 in the 1-km land cover data sets. Also, NDVI and land cover data sets at 1-km resolution may  
8 be insufficient to detect the phenology of the dominant crop in the administrative units.

9 In China Yunnan (code 126), we observe disagreements between SACRA and MIRCA. In  
10 China Yunnan, we observe that some of the grids have bimodal NDVI-Crop (black lines) in  
11 Fig. 11. It is possible that NDVI-Crop represents a mixed phenology of non-dominant and  
12 voluntary crops. Our approach is unable to consider a mixture of phenology. This may explain  
13 the disagreement between SACRA's sowing dates and those of other products.

14 A major discrepancy in crop calendars between SACRA and other products can be due to  
15 the selection of one dominant crop in each administrative unit. It is possible that SACRA  
16 detects the CC of similar maximal harvested area or another sub-crop in MIRCA2000 (e.g.,  
17 for irrigated wheat in India Uttar Pradesh with two identical areas with different cropping  
18 periods; cf. Table I-211 of Appendix I in Portmann, 2011). The disadvantages of our  
19 approach may be reduced with future improvements based on finer satellite sensors to avoid  
20 mixture of phenology from other crops and vegetation, and crop type classification studies to  
21 consider several dominant crops in each grid.

22 Taking into account the extreme disagreement between SACRA and MIRCA2000/W12 in  
23 some regions (Table 5 and Fig. 10), it becomes important to determine which CC is more  
24 reliable. However, it is difficult to decide which data set is more accurate in global studies.  
25 For example, the identification of the wheat type (sowing in spring or autumn) is difficult, as  
26 shown in disagreements among the three products in 12 administrative units (Table 5). Also,  
27 it is possible that both are correct, e.g., if they referred to different time periods. MIRCA2000  
28 possibly used the conditions of nearby administrative units because of a lack of more detailed  
29 reference information. Therefore, it is difficult to determine the absolute accuracy of the  
30 products through comparison. However, combined application of several products is useful to  
31 take the uncertainty of the CC into account. Since SACRA, MIRCA and W12 detect the CC  
32 from different approaches, a comparison of their results is useful for cross-validation.

### 1 **3.3 Advantages and disadvantages of SACRA**

2 This subsection discusses the advantages and disadvantages of SACRA compared to two  
3 other approaches: census-based and model-based methods. Additionally, this subsection also  
4 discusses possible improvements of SACRA. Table 6 summarizes the advantages and  
5 disadvantages of the census-based methods, model-based methods, and SACRA.

6 An advantage of SACRA is its fine spatial resolution compared to the other two data sets.  
7 Therefore, different CCs in the same administrative unit are considered in SACRA (Fig. 9a-  
8 2). The model-based method can also result in a variety of CCs. However, it is difficult to  
9 demonstrate that the variability is correct around the globe without knowledge of local CC  
10 information.

11 The spatial resolution of SACRA is equal to the maximum resolution of the satellite-  
12 sensed NDVI and the crop classification map. At present, NDVI from the moderate-resolution  
13 imaging spectroradiometer (MODIS) is available at a spatial resolution of 250 m (e.g., Zhang  
14 et al., 2006). However, present studies provide global crop classification maps at a spatial  
15 resolution of 5 arc-min (e.g., Monfreda et al., 2008; Portmann et al., 2010). Present land cover  
16 data sets, such as GLCC and Ecoclimap, only contain a small number of coarse agricultural  
17 classes. At the regional scale, many studies have been performed to classify crops using  
18 satellite-sensed data (e.g., Mingwei et al., 2008; Wardlow and Egbert, 2008; Wardlow et al.,  
19 2007). In this study, we use the crop classification map from MIRCA2000 at a spatial  
20 resolution of 5 arc-min. SACRA can be recalculated with higher resolution remote sensing  
21 data (e.g., from future Sentinel-2 data; Drusch et al., 2012) if higher resolution land cover  
22 maps become available. The higher resolution CC products can contribute to  
23 hydrological/agricultural studies which aim to conduct simulations at spatial resolution of 1  
24 km (e.g., Wood et al., 2011; Kotsuki et al., 2015).

25 A second advantage of SACRA is its easy detection of cultivation using time series of  
26 NDVI. Because agriculture is controlled by human decisions, it is difficult to estimate from  
27 the census-based and model-based methods whether or not farmers actually perform  
28 cultivation. Additionally, agriculture is affected by disasters, such as droughts, inundations,  
29 heat waves, and cool summer damages. The satellite-sensed NDVI can be used to detect  
30 whether the managed land is currently being cultivated or is temporarily in disuse. It is also  
31 possible to identify cropping intensity with time series of NDVI (Fig. 5).

1        However, SACRA has the disadvantage that it is inapplicable to future simulations such as  
2 impact assessments of climate change because SACRA is produced using past observational  
3 data. Future changes in agricultural water demand and biomass production are major issues in  
4 assessment studies of climate change (Hanjra and Qureshi, 2010). An advantage of SACRA  
5 compared to MIRCA2000 is that SACRA provides not only sowing/harvesting dates but also  
6 the peak date from the time series of NDVI. The peak date can be used to calibrate the  
7 parameters of crop growth models that simulate the growing stage during cultivation (e.g.,  
8 Horie 1987). SACRA can contribute to future assessment studies indirectly by being utilized  
9 to calibrate their model parameters.

10        It should be noted that our method is unsuitable for detecting the sowing dates of snow-  
11 wheat. Furthermore, our algorithm carries the possibility of overestimating or underestimating  
12 cultivation periods in the first estimation. Therefore, we adjusted the length of the cultivation  
13 period of SACRA to MIRCA2000. For the temperate crops, sowing and harvesting dates are  
14 moved (advanced/postponed) to adjust to the cultivation period. For snow-wheat, sowing date  
15 is defined with respect to the cultivation period of MIRCA2000 and the harvesting date of the  
16 first estimation. The adjustment indicates that the cultivation period of SACRA completely  
17 relies on that of MIRCA2000. However, the cultivation period can be different in the same  
18 administrative unit because of different climate. We plan to utilize both census-based and  
19 model-based cultivation period for the adjustment. Also, utilization of snow-cover products  
20 from satellite (e.g., MODIS snow cover product; Hall et al., 2002) or land surface data  
21 assimilation (e.g., global land data assimilation system; Rodel et al., 2004) would help to  
22 adjust the sowing date of snow-wheat appropriately.

23        Our method has the disadvantage that the mixture of several crops in a grid is not  
24 considered. Therefore, we assume that the NDVI-Crop represents the phenology of the  
25 dominant crop at each grid. Because of this assumption, our approach contains the following  
26 disadvantages: 1) The census-based and model-based approaches can contain CCs for more  
27 than one crop for every unit (e.g., MIRCA2000 and W12), while SACRA only contains the  
28 CC for the dominant crop in a given unit; 2) Census-based data can deliver a CC for either  
29 irrigated or rain-fed crops, while SACRA cannot separate them. In fact, CCs for irrigated and  
30 rain-fed cropland can be different; 3) Our approach cannot consider the mixture of phenology  
31 from several crops and voluntary crops. It should be also noted that the length of the  
32 cultivation period in SACRA is adjusted to MIRCA2000 to avoid the unrealistic cultivation



1 periods. A major discrepancy in crop calendars between SACRA and other products can be  
2 due to the selection of one dominant crop in each administrative unit. The disadvantages of  
3 our approach would be reduced with future improvements based on finer satellite sensors and  
4 crop type classification studies to consider several dominant crops in each administrative unit.

5 The idea behind CC estimation in SACRA is very simple, and therefore easily applicable  
6 to the global cropland and additional satellite observations. Due to data scarcity, we resort to  
7 averaged data from three consecutive years (2004–2006). The data product generated from  
8 this study therefore is of limited use for the direct parameterization of global growth models.  
9 However, taking into account the current development in Earth observation (e.g., the  
10 development of the European Space Agency’s Sentinel series), data scarcity will soon be less  
11 of an issue. The proposed method represents a simple and thus easily applied approach that  
12 can potentially make use of large amounts of temporally, highly-resolved, global, optical,  
13 Earth observation data and may provide interesting input parameters for global land surface  
14 models. For example, the estimation of an annual crop calendar is a major part of our scope.

15 Finally, the accuracy of SACRA depends on the accuracy of the NDVI and land cover data  
16 sets. The wavelengths required for the calculation of the NDVI are relatively easy to measure  
17 from satellite sensors. Therefore, the accuracy of the NDVI largely depends on the temporal  
18 resolution of adequate observations (e.g., the revisiting time of the applied systems and  
19 weather at satellite observation, such as cloud cover). Usage of several satellite sensors (e.g.,  
20 MODIS) would help to reduce the uncertainty of the NDVI. With respect to the accuracy of  
21 land cover data, we combine two land cover data sets to reduce the uncertainty of the land  
22 cover data. The land cover data sets, however, contain uncertainties (Herold et al., 2008;  
23 Nakaegawa, 2011). The land cover data sets could be improved by developing new  
24 algorithms, increasing the amount of supervised data, and utilizing multi-spectrum  
25 information. Further improvements of the land cover data sets would contribute to  
26 improvement of SACRA.

#### 27 **4 Summary**

28 This study aimed at producing a new crop calendar, SACRA, using satellite-sensed NDVI.  
29 This paper describes the methods to produce SACRA from the following four data sets: time  
30 series of NDVI, land cover data sets, reanalysis temperature, and census monthly agricultural  
31 data. The resulting SACRA data set included three products at a spatial resolution of 5 arc-  
32 min: (1) the spatial distribution of the dominant crop in major and second cultivation seasons;

1 (2) time series of NDVI of the cropland; (3) sowing, peak, and harvesting dates of the  
 2 dominant crop. The advantages and disadvantages of SACRA compared to other global crop  
 3 calendars are summarized as follows.

4 First, an advantage of SACRA is its finer spatial resolution compared to other existing  
 5 global crop calendars. However, a disadvantage is that the mixture of several crops in a grid  
 6 is not considered in SACRA. Second, the cultivation period of SACRA is identified from the  
 7 time series of NDVI, which corresponds to vegetation vitality. Therefore, SACRA considers  
 8 current effects of human decisions and natural disasters. Satellite-sensed NDVI data enable  
 9 detection of whether the managed land is currently cultivated or temporarily in disuse.  
 10 Finally, SACRA is inapplicable to future simulations because it is based on Earth observation  
 11 data. However, SACRA can potentially be used to calibrate the parameters of crop growth  
 12 models. An advantage of SACRA compared to census-based crop calendars is that SACRA  
 13 provides not only sowing/harvesting dates but also a peak date from the time series of NDVI  
 14 data.

15 Many improvements to SACRA are possible. For example, estimation of annual crop  
 16 calendars is a major part of our scope. We have made SACRA data sets available on our web  
 17 page free of charge. We encourage researchers to utilize our data and provide feedback on  
 18 errors or possible improvements.

## 19 **Appendix A: Calibration of crop calendar parameters**

20 This appendix describes the scheme used to calibrate two crop calendar parameters  
 21 ( $nNDVI_{sw}$  and  $nNDVI_{hv}$ ) from NDVI-Pure in Subsection 2.3. Once two parameters are given,  
 22 the sowing/harvesting dates are uniquely determined with Eq. (6). We calibrated the two CC  
 23 parameters so as to minimize the error between the determined and MIRCA2000 sowing  
 24 (harvesting) dates among calibration grids. Here, the error for the sowing (harvesting) date is  
 25 calculated by:

$$26 \quad \begin{aligned} ERR_{sw(hv)} = 0 & \quad \text{if} \quad Mon_{sw(hv),1st} \leq t_{sw,hv} \leq Mon_{sw(hv),End} \\ & \quad \text{else} \quad ERR_{sw(hv)} = \min \left( \left| t_{sw(hv)} - Mon_{sw(hv),1st} \right|, \left| t_{sw(hv)} - Mon_{sw(hv),End} \right| \right) \end{aligned} \quad (A1)$$

27 where,  $ERR$ ,  $t$ , and  $Mon$  denote error at the grid (day), sowing (or harvesting) dates (day of  
 28 year) determined by  $nNDVI_{sw}$  (or  $nNDVI_{hv}$ ), and sowing (or harvesting) month defined in  
 29 MIRCA2000.  $Mon_{1st(End)}$  denotes 1st (or end) dates of the month (day of year). Subscripts  $sw$ ,  
 30 and  $hv$  denote sowing and harvesting dates, respectively. By changing  $nNDVI_{sw}$  and  $nNDVI_{hv}$

1 from 0.01 to 1.0 with a 0.01 increment, we minimized the averaged  $ERR_{sw}$  and  $ERR_{hv}$  among  
2 calibration grids for each crop (Fig. A1). Note that  $nNDVI_{sw}$  of snow-wheat is not calibrated  
3 in this study since our method is unsuitable for estimation of sowing dates of snow-wheat  
4 (Subsection 2.3). The global distribution of calibration grids for six crops is shown in Fig. A2.

## 5 **Appendix B: Comparison of sowing dates**

6 This appendix aims to illustrate the differences in sowing dates of the three data sets:  
7 SACRA, MIRCA2000 (Portmann et al., 2010), and Waha et al. (2012), to supplement  
8 discussions in Subsection 3.2. Fig. A3 is similar to Fig. 9, but shows the differences in sowing  
9 dates for five specific crops (wheat, maize, rice, soybean, and cotton). Fig. A4 shows the  
10 cultivation seasons of the three products in 16 administrative units in Table 5. Since Waha et  
11 al. (2012) estimated only the sowing dates, we apply the cultivation period of MIRCA2000 at  
12 each administrative unit for purposes of illustration. The cultivation period of SACRA was  
13 also adjusted by that of MIRCA2000 (see Subsection 2.4 for details). Therefore, the three  
14 products have the same cultivation period in each administrative unit in Fig. A4.

## 15 **Acknowledgements**

16 Dr. K. Waha kindly provided the valuable data on sowing dates. We gratefully  
17 acknowledge two anonymous referees for their invaluable and constructive suggestions. This  
18 study was supported in part by the Japan Society for Promotion Science (JSPS) KAKENHI  
19 grants 12J03816, 22246066, 15K18128 and the SOUSEI Program of the Ministry of  
20 Education, Culture, Sports, Science, and Technology.

## 21 **References**

- 22 Döll, P., and Siebert, S.: Global modeling of irrigation water requirements. *Water Resour. Res.*,  
23 38, 1037, doi:10.1029/2001WR000355, 2002.
- 24 Drusch, M., Del Bello, U., Carlier, S., Colin, O., Fernandez, V., Gascon, F., Hoerschb, B.,  
25 Isolaa, C., Laberintia, P., Martimorta, P., Meygrete, A., Spotoa, F., Sya, O., Marchesed,  
26 F., and Bargellini, P.: Sentinel-2: ESA's optical high-resolution mission for GMES  
27 operational services. *Remote Sens. Environ.*, 120, 25–36, doi: 10.1016/j.rse.2011.11.026,  
28 2012.
- 29 Dye, D. G., and Tucker, C. J.: Seasonality and trends of snow - cover, vegetation index, and  
30 temperature in northern Eurasia. *Geophys. Res. Lett.*, 30, 1405, doi:  
31 10.1029/2002GL016384, 2003.

- 1 Food and Agriculture Organization of the United Nations: Bread wheat. FAO Plant  
2 Production and Protection Series 30. Rome, Italy. available at:  
3 <http://www.fao.org/docrep/006/y4011e/y4011e04.htm>
- 4 Faroux, A., Kaptuè Tchuentè, A. T., Roujean, J.-L., Masson, V., Maritin, E., and Le Moigne,  
5 P.: ECOCLIMAP-II/Europe: a twofold database of ecosystems and surface parameters at  
6 1 km resolution based on satellite information for use in land surface, meteorological and  
7 climate models. *Geosci. Model Dev.*, 6, 563–582, doi: 10.5194/gmd-6-563-2013, 2013.
- 8 Fischer, G., Velthuizen, H., and Nachtergaele, F.: Global Agro-Ecological Zones Assessment:  
9 Methodology and Results. Interim report. Luxemburg, Austria: International Institute for  
10 Systems Analysis (IIASA), and Rome: FAO, 2000.
- 11 Hall, D. K., Riggs, G. A., Salomonson, V. V., DiGirolamo, N. E., and Bayr, K. J.: MODIS  
12 snow-cover products. *Remote Sens. Environ.*, 83, 181-194, doi: 10.1016/S0034-  
13 4257(02)00095-0, 2002.
- 14 Hanasaki, N., Kanae, S., Oki, T., Masuda, K., Motoya, K., Shirakawa, N., Shen, Y., and  
15 Tanaka, K. An integrated model for the assessment of global water resources. –Part 2:  
16 Applications and assessments. *Hydrol. Earth Syst. Sci.*, 12, 1027–1037,  
17 doi:10.5194/hess-12-1027-2008, 2008.
- 18 Hanjra, M. A., and Qureshi, M. E. Global water crisis and future food security in an era of  
19 climate change. *Food Policy*, 35, 365–377, doi:10.1016/j.foodpol.2010.05.006, 2010.
- 20 Herold, M., Mayaux, P., Woodcock, C. E., Baccini, A., and Schmullius, C.: Some challenges  
21 in global land cover mapping : An assessment of agreement and accuracy in existing 1  
22 km datasets, *Remote Sens. Environ.*, 112, 2538–2556, doi:10.1016/j.rse.2007.11.013,  
23 2008.
- 24 Hirabayashi, Y., Kanae, S., Motoya, K., Masuda, K., and Petra, D.: A 59-year (1948–2006)  
25 global near-surface meteorological data set for land surface models. Part I : Development  
26 of daily forcing and assessment of precipitation intensity, *Hydrol. Res. Lett.*, 2, 36–40,  
27 doi:10.3178/HRL.2.36, 2008.
- 28 Horie T. A model for evaluating climate productivity and water balance of irrigated rice and  
29 its application to Southeast Asia. *Southeast Asian Studies* 25: 62–74, 1987.
- 30 Kotsuki, S., Takenaka, H., Tanaka, K., Higuchi, A., and Miyoshi, T.: 1-km-resolution land  
31 surface analysis over Japan: Impact of satellite-derived solar radiation. *Hydrol. Res. Lett.*,  
32 9, 14–19, doi: 10.3178/hr.9.14, 2015.
- 33 Krysanova, V., Wechsung, F., Arnold, J., Srinivasan, R., and Williams, J.: SWIM (Soil and  
34 Water Integrated Model) User Manual. Potsdam Institute for Climate Impact Research,  
35 Potsdam, Germany, 2000.
- 36 Loveland, T. R., Reed, B. C., Brown, J. F., Ohlen, D. O., Zhu, Z., Yang, L., and Merchant, J.  
37 W.: Development of a global land cover characteristics database and IGBP DISCover

- 1 from 1 km AVHRR data. *Int. J. Remote Sens.*, 21, 1303–1330, doi:  
2 10.1080/014311600210191, 2000.
- 3 Maisongrande, P., Duchemin, B., and Dedieu, G.: VEGETATION/SPOT: an operational  
4 mission for the Earth monitoring; presentation of new standard products. *Int. J. Remote*  
5 *Sens.*, 25, 9–14, doi:10.1080/0143116031000115265, 2004.
- 6 Mingwei, Z., Qingbo, Z., Zhongxin, C., Jia, L., Yong, Z., and Chongfa, C.: Crop  
7 discrimination in Northern China with double cropping systems using Fourier analysis of  
8 time-series MODIS data. *Int. J. Appl. Earth Obs. Geoinf.*, 10, 476–485,  
9 doi:10.1016/j.jag.2007.11.002, 2008.
- 10 Monfreda, C., Ramankutty, N., and Foley, J.: Farming the planet: 2. Geographic distribution  
11 of crop areas, yields, physiological types, and net primary production in the year 2000.  
12 *Global Biogeochem. Cy.*, 22, 1–19, doi:10.1029/2007GB002947, 2008/
- 13 Nakaegawa, T.: Comparison of Water-Related Land Cover Types in Six 1-km Global Land  
14 Cover Datasets. *J. Hydrometeorol.*, 13, 649–664, doi:10.1175/JHM-D-10-05036.1, 2012.
- 15 Pokhrel, Y., Hanasaki, N., Koirala, S., Cho, J., Yeh, P., Kim, H., Kanae, S., and Oki, T.:  
16 Incorporating Anthropogenic Water Regulation Modules into a Land Surface Model. *J.*  
17 *Hydrometeorol.*, 13, 255–269, doi:10.1175/JHM-D-11-013.1, 2012.
- 18 Portmann, F., Siebert, S., and Döll, P.: MIRCA2000—Global monthly irrigated and rainfed  
19 crop areas around the year 2000: A new high - resolution data set for agricultural and  
20 hydrological. *Global Biogeochem. Cy.*, 24, 1–24, doi:10.1029/2008GB003435, 2010.
- 21 Portmann, F. : Global estimation of monthly irrigated and rainfed crop areas on a 5 arc-  
22 minute grid. *Frankfurt Hydrology Paper (09)*, 2011.
- 23 Pettorelli, N., Vik, J. O., Mysterud, A., Gaillard, J. M., Tucker, C. J., and Stenseth, N. C. :  
24 Using the satellite-derived NDVI to assess ecological responses to environmental change.  
25 *Trends in ecology & evolution*, 20, 503–510, doi: 10.1016/j.tree.2005.05.011, 2005.
- 26 Rockström, J., Falkenmark, M., Karlberg, L., Hoff, H., Rost, S., Gerten, D.: Future water  
27 availability for global food production: The potential of green water for increasing  
28 resilience to global change. *Water Resour. Res.*, 45, W00A12,  
29 doi:10.1029/2007WR006767, 2009.
- 30 Rodell, M., and Coauthors: The global land data assimilation system. *Bull. Amer. Meteor.*  
31 *Soc.*, 85, 381-394, doi: 10.1175/BAMS-85-3-381, 2002.
- 32 Rost, S., Gerten, D., Bondeau, A., Lucht, W., Rohwer, J., and Schaphoff, S.: Agricultural  
33 green and blue water consumption and its influence on the global water system. *Water*  
34 *Resour. Res.*, 44, W09405, doi:10.1029/2007WR006331, 2008.
- 35 Sacks, W. J., Deryng, D., Foley, J. A., and Ramankutty, N.: Crop planting dates: an analysis  
36 of global patterns. *Global Ecol. Biogeogr.*, 19, 607–620, doi:10.1111/j.1466-  
37 8238.2010.00551.x, 2010.

- 1 Sakamoto, T., Wardlow, B. D., Gitelson, A., Verma, S. B., Suyker, A. E., and Arkebauer, T.  
2 J.: A Two-Step Filtering approach for detecting maize and soybean phenology with time-  
3 series MODIS data. *Remote Sens. Environ.*, 114, 2146–2159,  
4 doi:10.1016/j.rse.2010.04.019, 2010.
- 5 Sakamoto, T., Yokozawa, M., Toritani, H., Shibayama, M., Ishitsuka, N., and Ohno, H.: A  
6 crop phenology detection method using time-series MODIS data. *Remote Sens. Environ.*,  
7 96, 366–374, doi:10.1016/j.rse.2005.03.008, 2005.
- 8 Siebert, S., and Döll, P.: Quantifying blue and green virtual water contents in global crop  
9 production as well as potential production losses without irrigation. *J. Hydrol.*, 384, 198–  
10 217, doi:10.1016/j.jhydrol.2009.07.03, 2010.
- 11 Stehfest, E., Heistermann, M., Priess, J. A., Ojima, D. S., and Alcamo, J.: Simulation of  
12 global crop production with the ecosystem model DayCent. *Ecol. Modelling*, 209, 203-  
13 219, doi: 10.1016/j.ecolmodel.2007.06.028, 2007.
- 14 Tan, G., and Shibasaki, R.: Global estimation of crop productivity and the impacts of global  
15 warming by GIS and EPIC integration. *Ecol. Modelling*, 168, 357-370, doi:  
16 10.1016/S0304-3800(03)00146-7, 2003.
- 17 Viovy, N., Arino, O., and Belward, A. S.: The Best Index Slope Extraction (BISE): A method  
18 for reducing noise in NDVI time-series. *Int. J. Remote Sens.*, 13, 1585–1590,  
19 doi:10.1080/01431169208904212, 1992.
- 20 Waha, K., Van Bussel, L. G. J., Müller, C., and Bondeau, A.: Climate - driven simulation of  
21 global crop sowing dates. *Global Ecol. Biogeogr.*, 21, 247-259, doi: 10.1111/j.1466-  
22 8238.2011.00678.x, 2012.
- 23 Wardlow, B., Egbert, S., and Kastens, J.: Analysis of time-series MODIS 250 m vegetation  
24 index data for crop classification in the U.S. Central Great Plains. *Remote Sens. Environ.*,  
25 108, 290–310, doi:10.1016/j.rse.2006.11.021, 2007.
- 26 Wood, E., and Coauthors: Hyperresolution global land surface modeling: Meeting a grand  
27 challenge for monitoring Earth’s terrestrial water. *Water Resour. Res.*, 47, W05301, doi:  
28 10.1029/2010WR010090, 2011.
- 29 Yorozu K., Tanaka K., Ikebuchi S.: Creating a global 1-degree dataset of crop type and  
30 cropping calendar through timeseries analysis of NDVI for GSWP simulation  
31 considering irrigation effect, *Proc. of 85th AMS Annual Meeting*, J6.8, 2005.
- 32 Zabel, F., Putzenlechner, B., and Mauser, W.: Global Agricultural Land Resources–A High  
33 Resolution Suitability Evaluation and Its Perspectives until 2100 under Climate Change  
34 Conditions. *PloS one*, 9, e107522, doi:10.1371/journal.pone.0107522, 2014.
- 35 Zhang, X., Friedl, M., and Schaaf, C. B.: Global vegetation phenology from Moderate  
36 Resolution Imaging Spectroradiometer (MODIS): Evaluation of global patterns and  
37 comparison with in situ measurements. *J. Geophys. Res.*, 111, G04017,  
38 doi:10.1029/2006JG000217, 2006.

1 Table 1. Characteristics and sources of the four global input data sets.

<b>Data</b>	<b>Source</b>	<b>Detailed description</b>
NDVI (1 km $\approx$ 30 seconds)	VEGETATION/SPOT	Maisongrande et al. (2004)
Land cover (30 seconds)	GLCC version 2.0	Loveland et al. (2000)
	Ecoclimap version 2.0	Faroux et al. (2013)
Census-based crop classification (5 arc-min) and crop calendar (5 arc-min)	MIRCA2000	Portmann et al. (2010)
Temperature (0.5 degree)	H08	Hirabayashi et al. (2008)

2

3

1 Table 2. List of crops. Checkmarks denote crops used for (a) estimation of crop calendar and  
 2 (b) comparison of cropping intensity.

ID	Crop name	(a) Calendar	(b) Intensity	ID	Crop Name	(a) Calendar	(b) Intensity
1	Temperate-wheat	✓	✓	10	Millet		✓
2	Snow-wheat	✓	✓	11	Oil palm		✓
3	Maize	✓	✓	12	Potato		✓
4	Rice	✓	✓	13	Rapeseed		✓
5	Soybean	✓	✓	14	Rye		✓
6	Cotton	✓		15	Sorghum		✓
7	Barley		✓	16	Sugarcane		✓
8	Cassava		✓	17	Sunflower		✓
9	Groundnuts		✓				

3

4



1 Table 3. Comparison of estimated cropping intensity in this study, Zabel et al. (2014), and  
 2 MIRCA2000 simplified cropping intensity for irrigated (IRC) and rain-fed (RFC) crop  
 3 classes in six administrative units (six boxes A–F in Figs. 5a and 5b). Averaged cropping  
 4 intensities over the administrative units are shown as “Cropping intensity”. “Code” and  
 5 “Crop” represents assigned code of the administrative unit in SACRA, and dominant crop  
 6 in major cultivation season in this study. The simplified cropping intensities are annual  
 7 harvested area divided by maximum monthly cropped area, which are defined for both  
 8 irrigated and rain-fed classes of 26 crop types.

Code	Box in Fig. 5	Name of administrative unit	Crop	Cropping intensity (yr <sup>-1</sup> )			
				This study	Zabel et al. (2014)	MIRCA IRC	MIRCA RFC
073	A	Brazil Rio Grande do Sul	MAZ	1.2	3.0	1.0	1.0
109	B	China Henan	SWH	2.2	1.0	1.0	1.0
157	C	France	SWH	1.3	1.0	1.0	1.0
211	D	India Uttar Pradesh	TWH	2.0	1.0	2.0	1.1
227	E	Kenya	MAZ	1.8	1.3	1.0	1.0
364	F	U. S. Mississippi	SOY	0.8	2.1	1.0	1.0

9 TWH: Temperate-wheat, SWH: Snow-wheat, MAZ: Maize, and SOY: Soybean.

10

1 Table 4. Number of calibration grids, calibrated two crop calendar parameters (nNDVI<sub>sw</sub> and  
 2 nNDVI<sub>hv</sub>), and averaged errors (nNDVI) in sowing/harvesting dates between determined  
 3 and MIRCA2000 among calibration grids of the six crop types.

	unit	Temp. wheat	Snow-wheat	Maize	Rice	Soybean	Cotton
Num. of grid	N	70	50	60	50	39	16
nNDVI <sub>sw</sub>	–	0.23	–	0.15	0.39	0.16	0.33
nNDVI <sub>hv</sub>	–	0.31	0.65	0.75	0.72	0.36	0.35
Error (sow)	day	15.5	–	9.7	12.5	13.0	19.4
Error (harvest)	day	19.9	23.4	8.2	3.2	12.8	11.5

4

5

1 Table 5. Administrative units with large absolute differences in sowing date ( $> 150$  days)  
2 between SACRA and MIRCA2000 or SACRA and Waha et al. (2012). SCR, MRC, and  
3 W12 in the table represent SACRA, MIRCA2000, and Waha et al. (2012), respectively.  
4 “Code” and “Crop” represent the assigned code of the administrative unit in SACRA, and  
5 the dominant crop in the major cultivation season in this study. The table compares  
6 sowing dates averaged over the administrative units. Only single cropping grids are used  
7 to compute the averaged sowing date for SACRA.

Code	Name of administrative unit	Crop	Sowing date (DOY)			Difference (days)	
			SCR	MRC	W12	SCR-MRC	SCR-W12
8	Azerbaijan	TWH	104.1	105	305.7	-0.9	163.4
36	AUS Queensland	TWH	1.7	166	341.6	-164.3	25
49	Bhutan	RIC	213.1	166	60.8	47.1	152.3
99	China Beijing	SWH	89.1	288	289.7	166.1	164.3
102	China Gansu	SWH	86.9	288	103	163.9	-16.1
107	China Hebei	SWH	84.5	288	316.4	161.5	133
109	China Henan	SWH	94.2	288	305.1	171.2	154
117	China Ningxia	SWH	76.3	288	48.6	153.3	27.7
119	China Shaanxi	SWH	103.6	288	292.8	180.6	175.7
120	China Shandong	SWH	83.7	288	300.8	160.7	148
122	China Shanxi	SWH	87.8	288	336.9	164.8	115.9
126	China Yunnan	MAZ	162	319	105.8	-157	56.2
192	IND Himachal Pradesh	SWH	157.3	319	135.2	-161.7	22
207	IND Sikkim	MAZ	195.5	166	31	29.5	164.5
225	Kazakhstan	SWH	286.6	258	105.1	28.6	181.5
394	Uruguay	RIC	175.2	349	294.8	-173.8	-119.6

TWH: Temperate-wheat, SWH: Snow-wheat, MAZ: Maize, RIC: Rice, COT: Cotton

AUS: Australia, IND: India

Blue colours: SCR is similar to MRC (< 90 days), but different from W12 (> 100 days)

Green colours: SCR is similar to W12 (< 90 days), but different from MRC (> 100 days)

Red colours: SCR is different from both MRC and W12 (> 100 days)

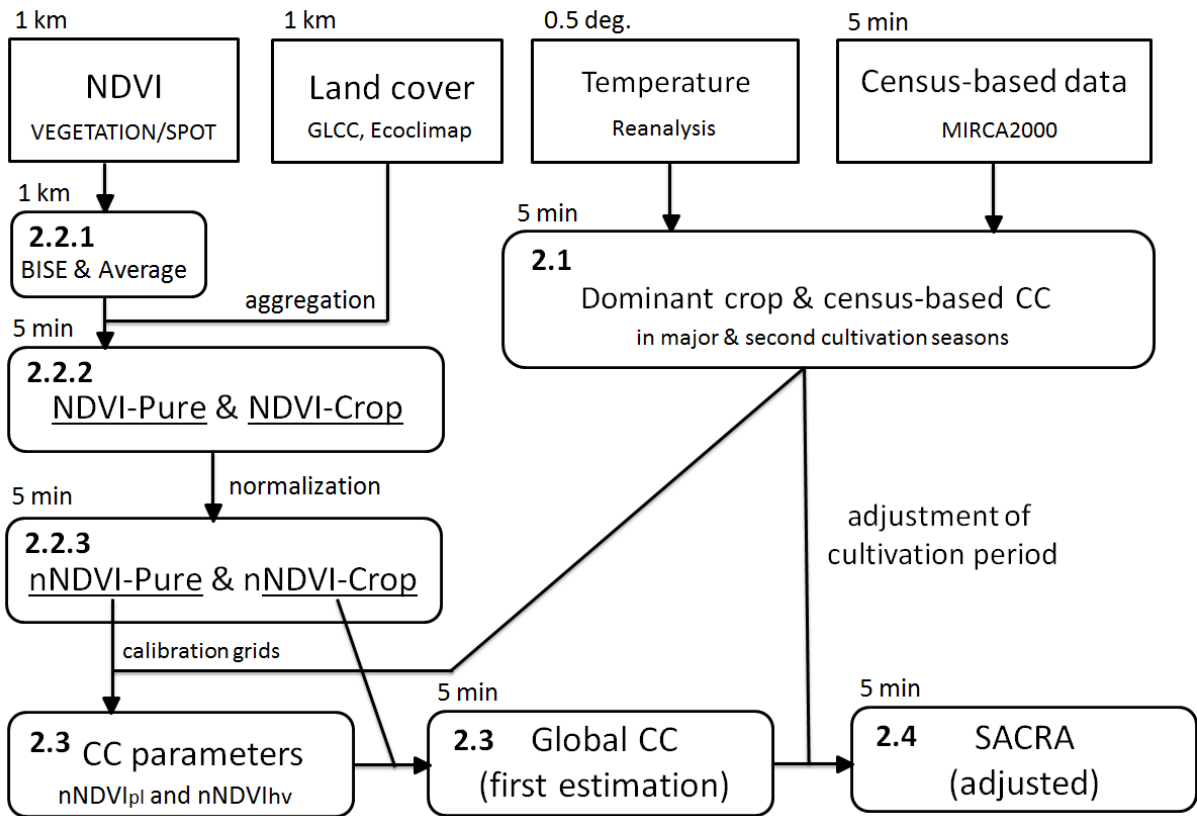
1  
2

1 Table 6. Advantages and disadvantages of three types of global crop calendars: census-based,  
 2 model-based, and Earth observation-based.

	Census-based	Model-based	Earth observation-based
Main inputs	Census data	Forcing data	Satellite-sensed NDVI
Resolution	Country/state scale	Equal to forcing data	5 arc-min
Different CC in a same admin. unit	impossible	possible	possible
Detection of cultivation	hard	hard	easy
Mixture of several crops in a grid	possible	possible	impossible
Application to future simulations	impossible	possible	impossible

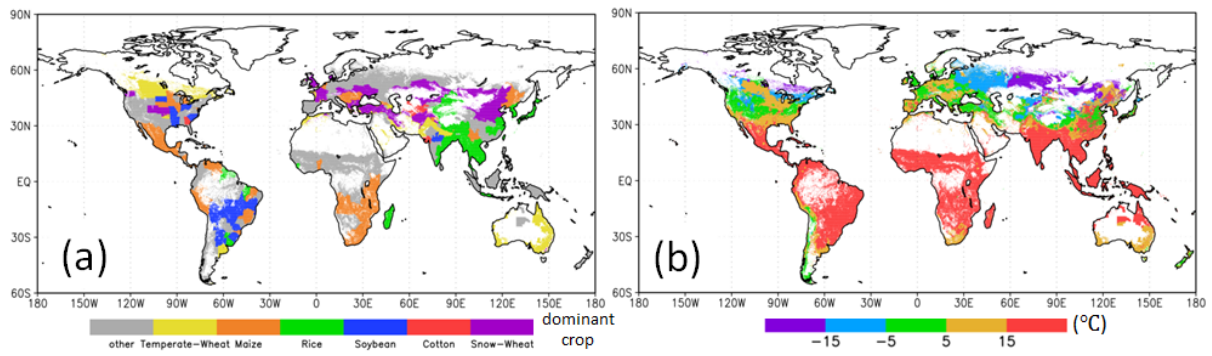
3

4



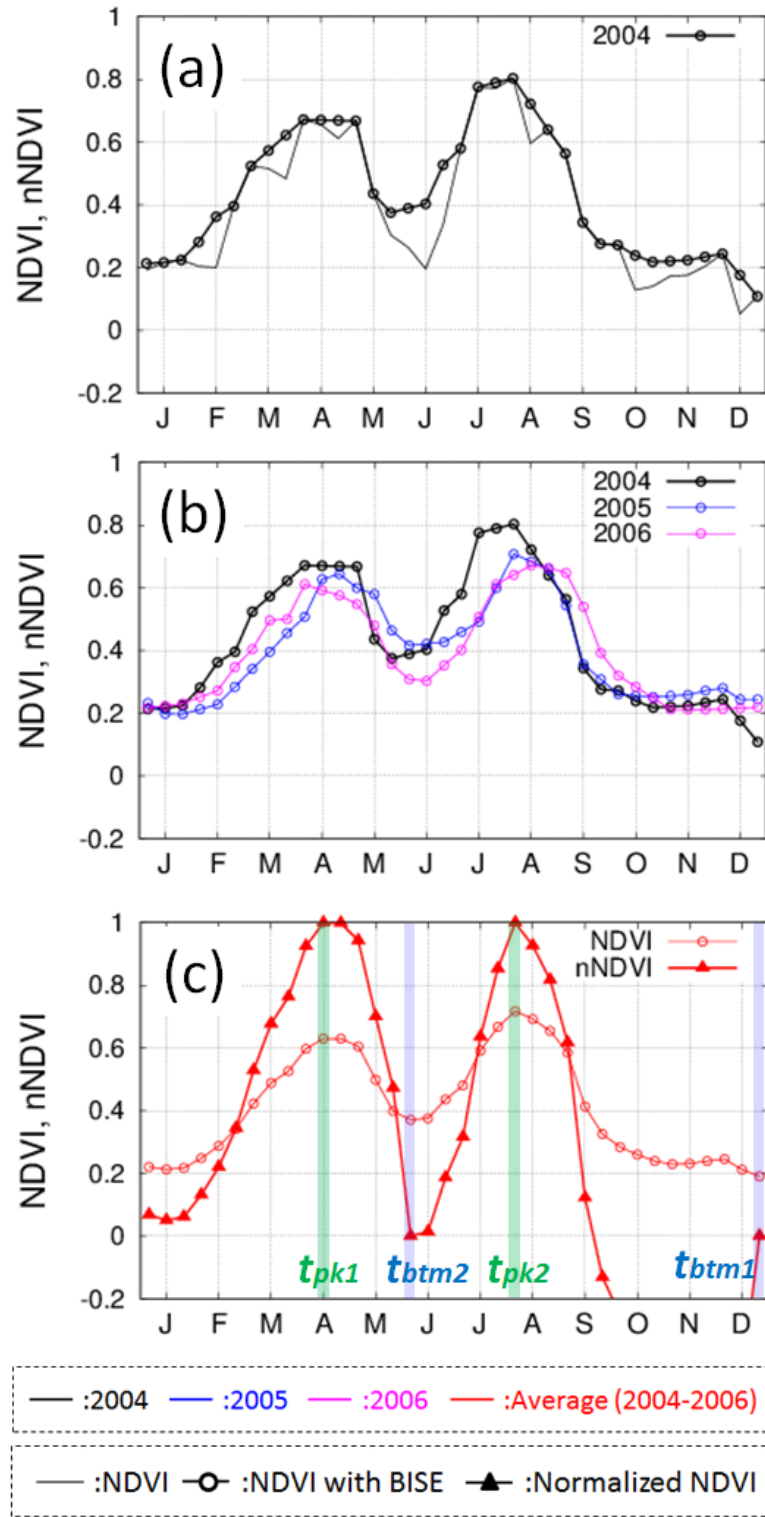
1  
2  
3  
4  
5  
6  
7

Fig. 1. Data processing scheme for the production of the global satellite-derived crop calendar (SACRA). The bold numbers inside the boxes indicate the subsections in this paper where the different processing steps are described. The numbers outside the boxes indicate the spatial resolution of the respective data sets. The top four boxes indicate input data (Table 1), and the other boxes indicate the results from our data processes.



1  
2  
3  
4  
5

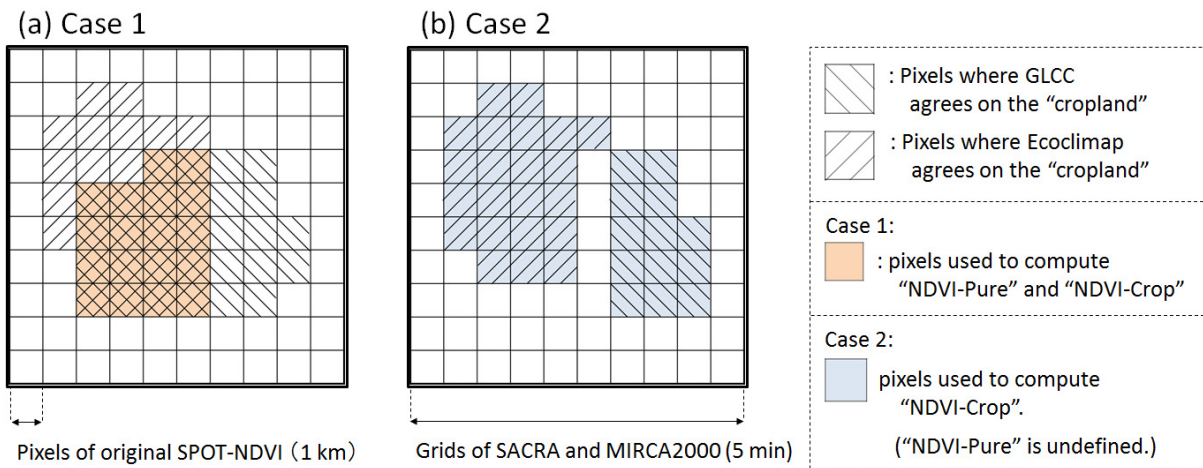
Fig. 2. Global distribution of (a) dominant crops in SACRA, and (b) minimum monthly-averaged temperature (°C) during the cultivation period of the dominant crops. Both panels represent the dominant crop in the major cultivation season.



1  
2  
3  
4  
5  
6

Fig. 3. Time series of NDVI at a double-cropping pixel in China (E116.76°, N32.60°). Panel (a) represents the original NDVI and NDVI with the BISE correction. Panel (b) represents the NDVI with the BISE correction from 2004 to 2006. Panel (c) represents NDVI average over 2004–2006, and normalized NDVI (nNDVI).

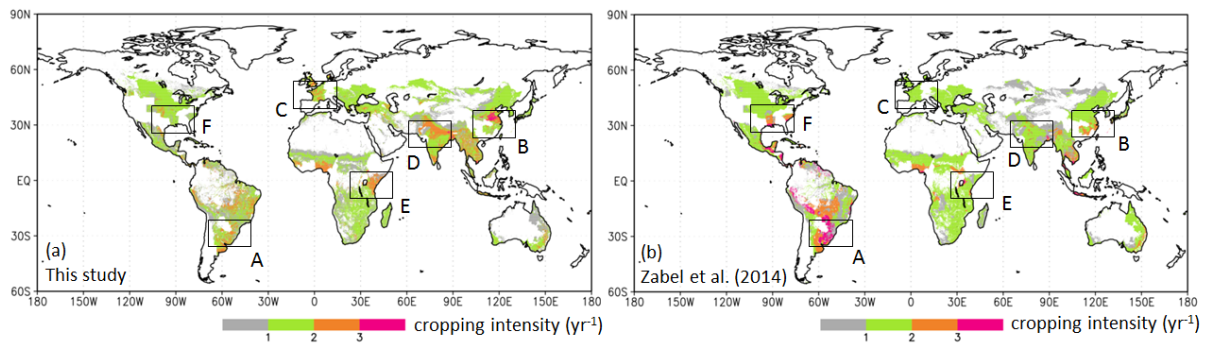




1

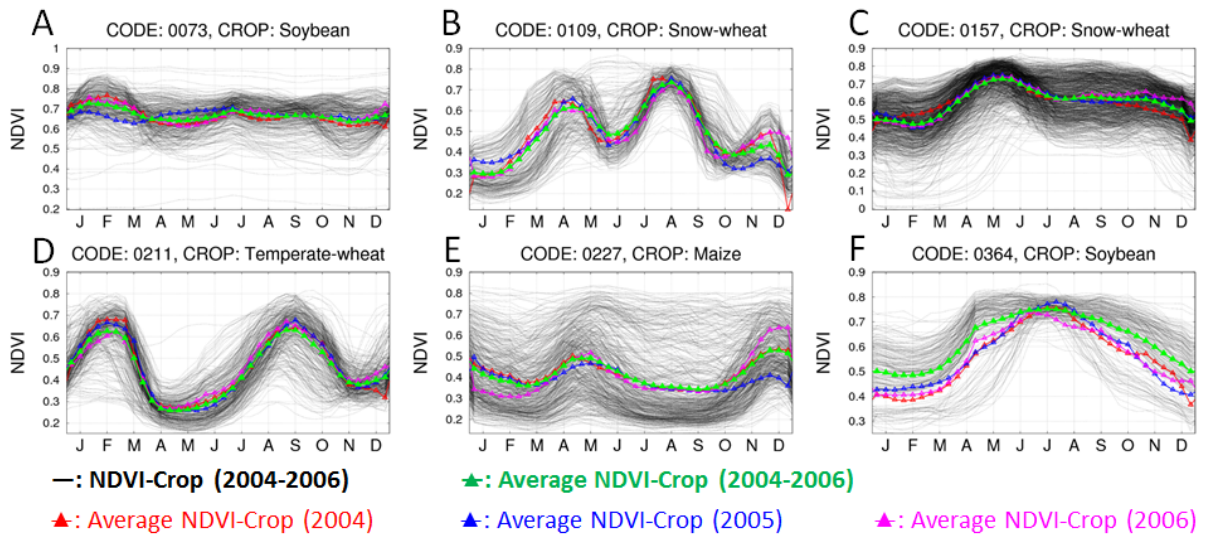
2 Fig. 4. Schematic image of the aggregation of NDVI-Pure and NDVI-Crop from 1-km-  
 3 resolution original NDVI. Small-sized squares with thin lines represent pixels of original  
 4 SPOT-NDVI (1-km-resolution). Large-sized squares with bold lines represent grids of  
 5 SACRA and MIRCA2000 (5 arc-min-resolution). Pixels with diagonal lines (from upper-  
 6 left to bottom-right and bottom-left to upper-right) show where GLCC and Ecoclimap  
 7 agree on the cropland.

8



1  
2  
3  
4  
5

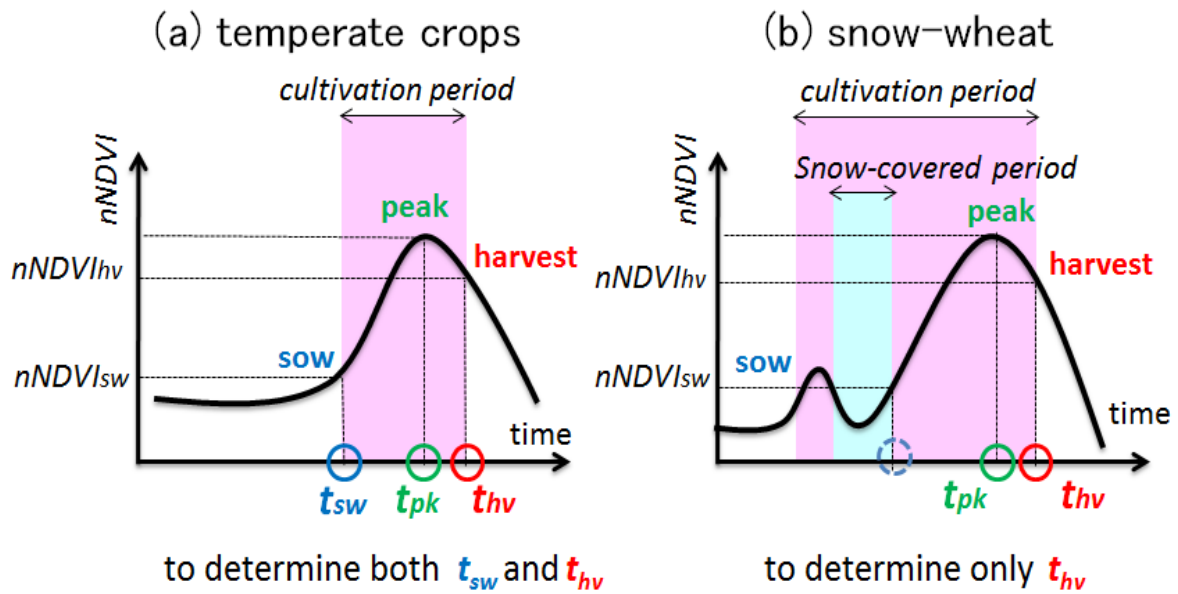
Fig. 5. Global distribution of (a) detected cropping intensity in this study, and (b) climate-based estimation of cropping intensity suitability (i.e., maximal cropping intensity; Zabel et al., 2014). The cropping intensity of the dominant crop is illustrated in Fig. 5(b).



1

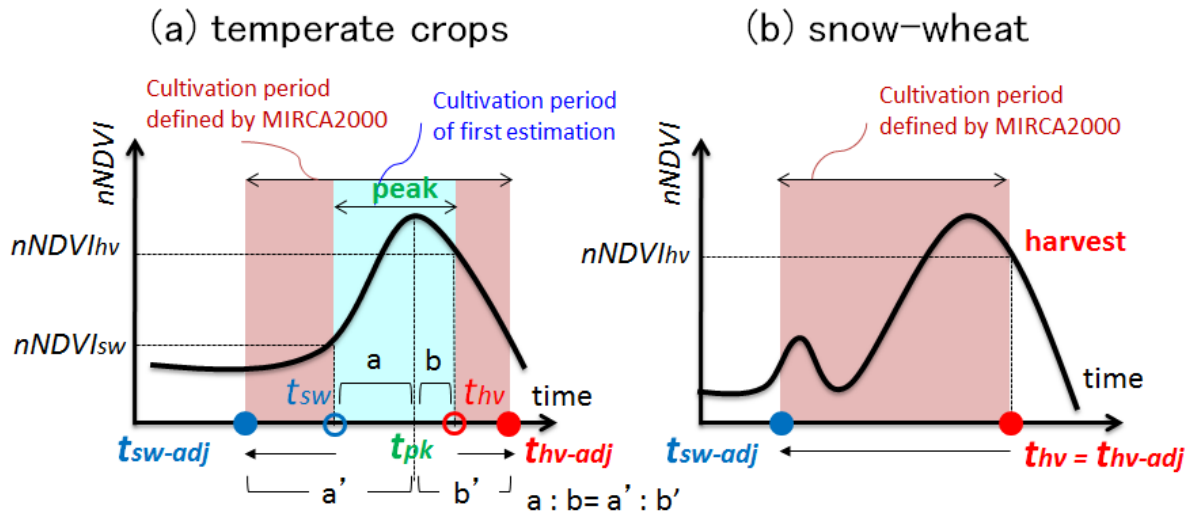
2 Fig. 6. Time series of NDVI for six administrative units in Table 3; Brazil Rio Grande do Sul  
 3 (code 73), China Henan (code 109), France (code 157), India Uttar Pradesh (code 211),  
 4 Kenya (code 227), and U. S. Mississippi (code 364). Black lines show time series of  
 5 NDVI-Crop averaged over 2004–2006 in the administrative units (i.e., NDVI of all grids  
 6 in the administrative units). Green lines show the average of black lines (i.e., averaged  
 7 over the administrative units). Red, blue, and magenta represent NDVI-Crop in 2004,  
 8 2005, and 2006, respectively, averaged over the administrative units.

9



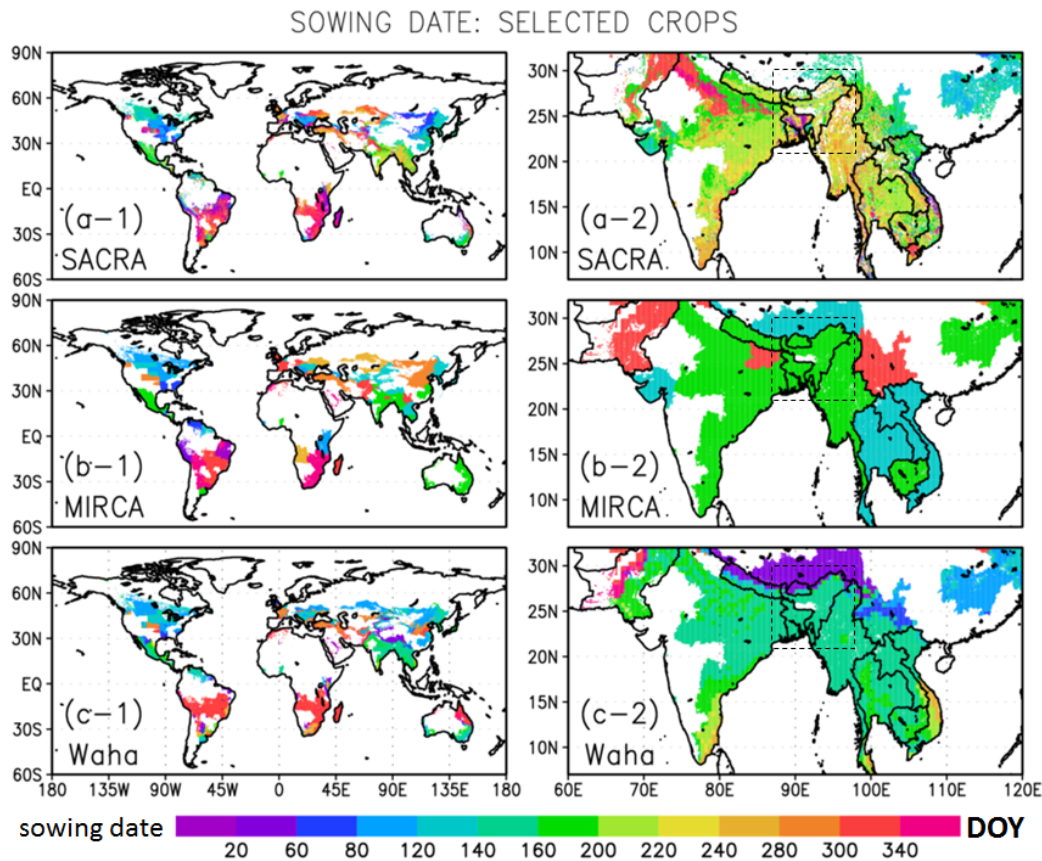
1  
2  
3  
4  
5  
6  
7  
8

Fig. 7. Scheme of identification of sowing and harvesting dates in this study. Sowing and harvesting dates ( $t_{sw}$  and  $t_{hv}$ ) are identified together with a vegetation index time series (black lines) and two crop calendar (CC) parameters:  $nNDVI_{sw}$  and  $nNDVI_{hv}$ . Figures (a) and (b) indicate temperate crops (temperate-wheat, maize, rice, soybean, and cotton) and snow-wheat, respectively. The two CC parameters are defined for the six crop types (Table 2a).



1  
 2 Fig. 8. Scheme used to adjust the cultivation period of SACRA to that of MIRCA2000.  $t_{sw}$   
 3 ( $t_{hv}$ ) and  $t_{sw-adj}$  ( $t_{hv-adj}$ ) denote sowing (harvesting dates) for the first estimation and  
 4 subsequent to the adjustment, respectively. For temperate crops, sowing and harvesting  
 5 dates are moved (advanced or postponed) to adjust the cultivation period to MIRCA2000.  
 6 In this treatment, the ratio of  $t_{pk}-t_{sw}$  to  $t_{hv}-t_{pk}$  is preserved as the ratio of  $t_{pk}-t_{sw-adj}$  to  $t_{hv-}$   
 7  $adj-t_{pk}$ . For snow-wheat, the harvesting date has not changed (i.e.,  $t_{hv}=t_{hv-adj}$ ). Sowing date  
 8 is determined by the cultivation period of MIRCA2000 and the harvesting date of the first  
 9 estimation.

10



1

2 Fig. 9. Sowing dates (unit: day of year) of dominant crops in the major cultivation season for

3 (a) SACRA, (b) MIRCA2000, and (c) Waha et al. (2012). Left panels (a-1, b-1, and c-1)

4 and right panels (a-2, b-2, and c-2) show global and South Asian maps, respectively.

5 Sowing dates are illustrated in grids where the dominant crop is temperate-wheat, snow-

6 wheat, maize, rice, soybean or cotton. The major seasons at multiple cropping grids are

7 determined by Eq. (7) for SACRA. Panels of SACRA contain sowing dates of major

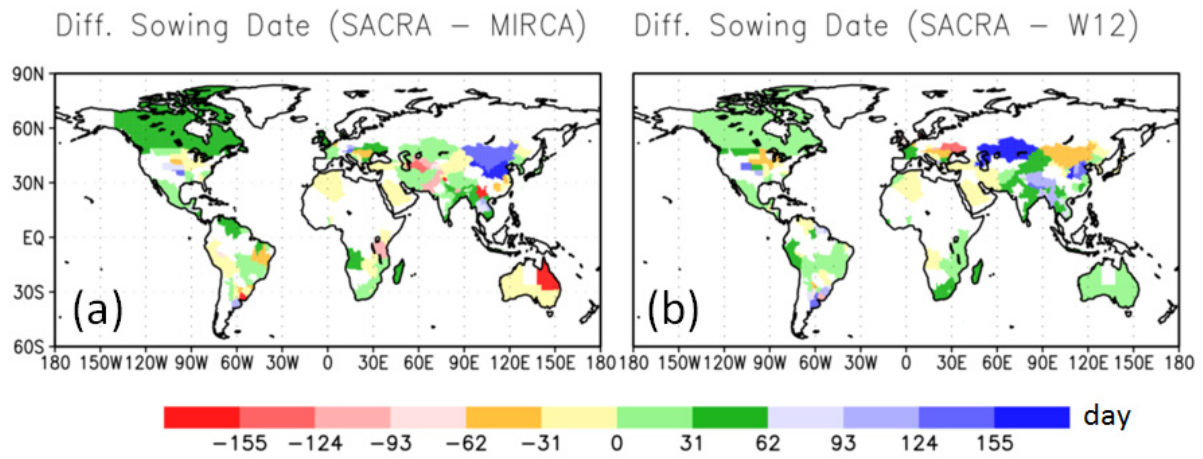
8 cultivation season for both single and multiple cropping grids. Boxes in right panels

9 represent the area where SACRA did not detect the crop calendar in some grids while

10 MIRCA2000 and Waha et al. (2012) defined.

11

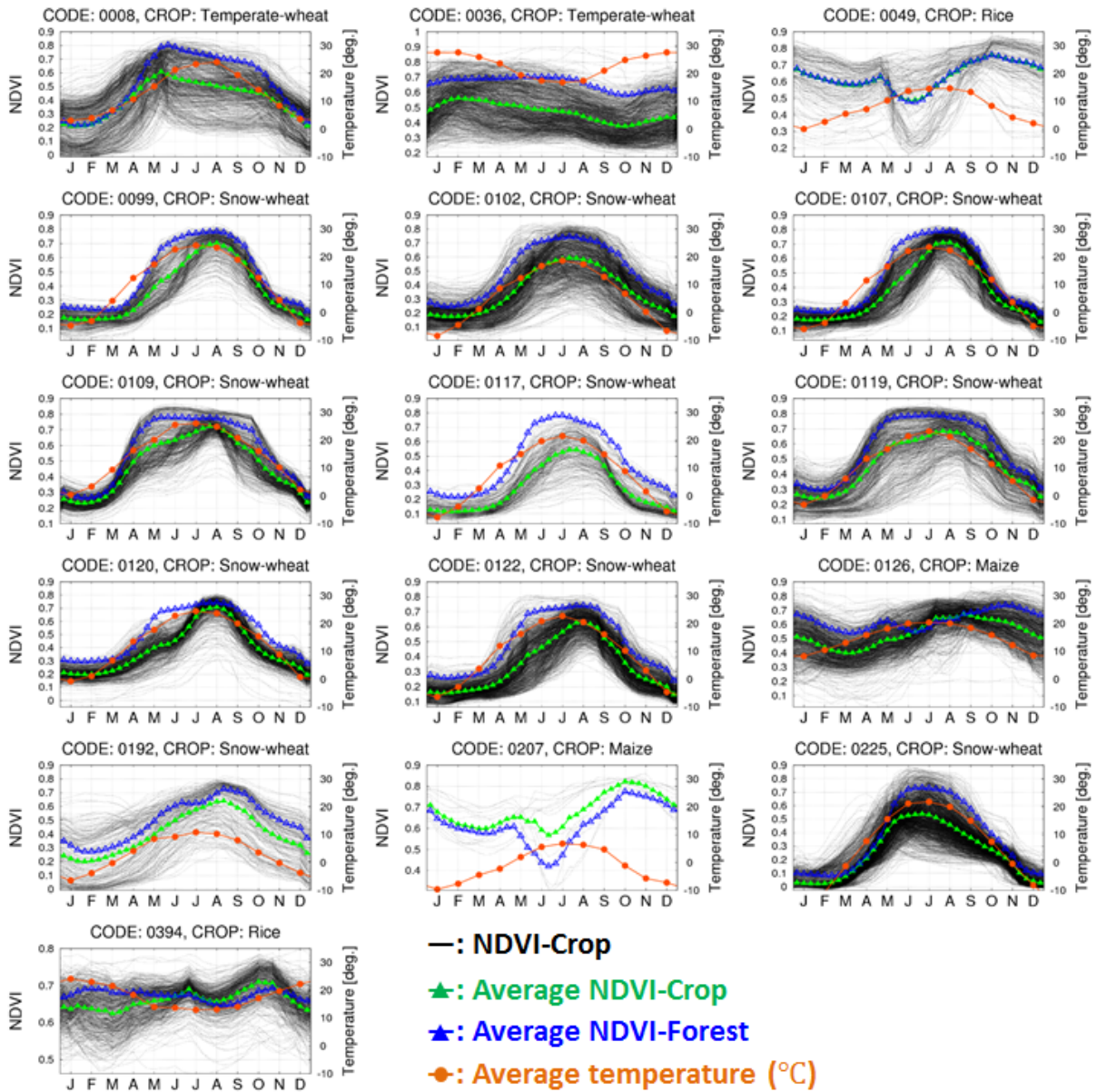
12



1  
2  
3  
4  
5  
6  
7  
8

Fig. 10. Differences in sowing dates of the dominant crop in the major cultivation season (a: SACRA–MIRCA2000; b: SACRA–Waha et al., 2012). The administrative units are illustrated if their dominant crop in the major cultivation season is temperate-wheat, snow-wheat, maize, rice, soybean or cotton. The differences for each specific crop type are shown in Fig. A3. Only single cropping grids are used to compute the averaged sowing date for SACRA





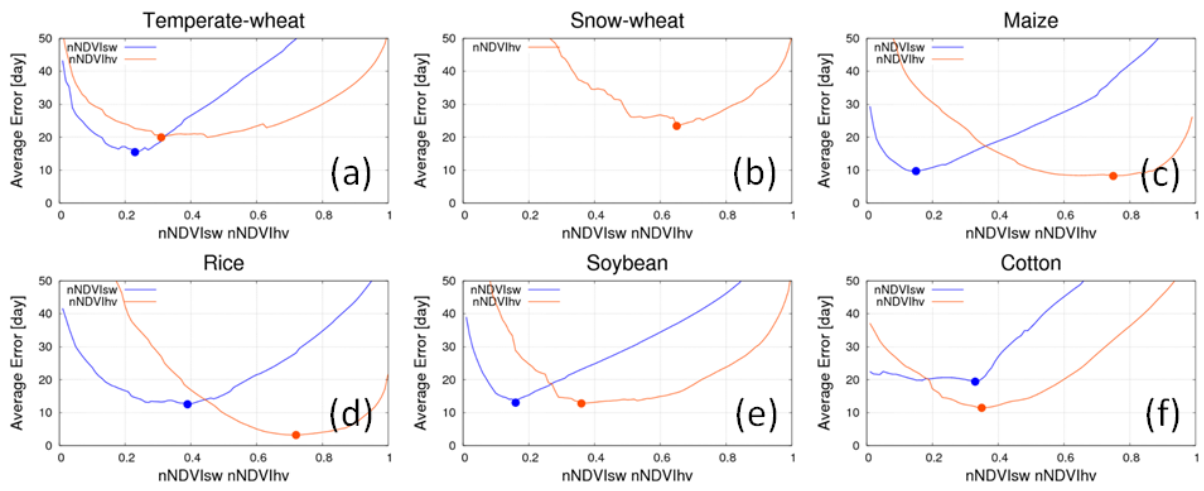
1

2

Fig. 11. Time series of the NDVI-Crop (black lines), average NDVI-Crop (green lines), average NDVI-Forest (blue lines), and average temperature (orange lines; °C) in the 16 administrative units in Table 5; Azerbaijan (code 8), Australia Queensland (code 36), Bhutan (code 49), China Beijing (code 99), China Gansu (code 102), China Hebei (code 107), China Henan (code 109), China Ningxia (code 117), China Shaanxi (code 119), China Shandong (code 120), China Shanxi (code 122), China Yunnan (code 126), India Himachal Pradesh (code 192), India Sikkim (code 207), Kazakhstan (code 225), and Uruguay (code 394). The average denotes average over the administrative units.

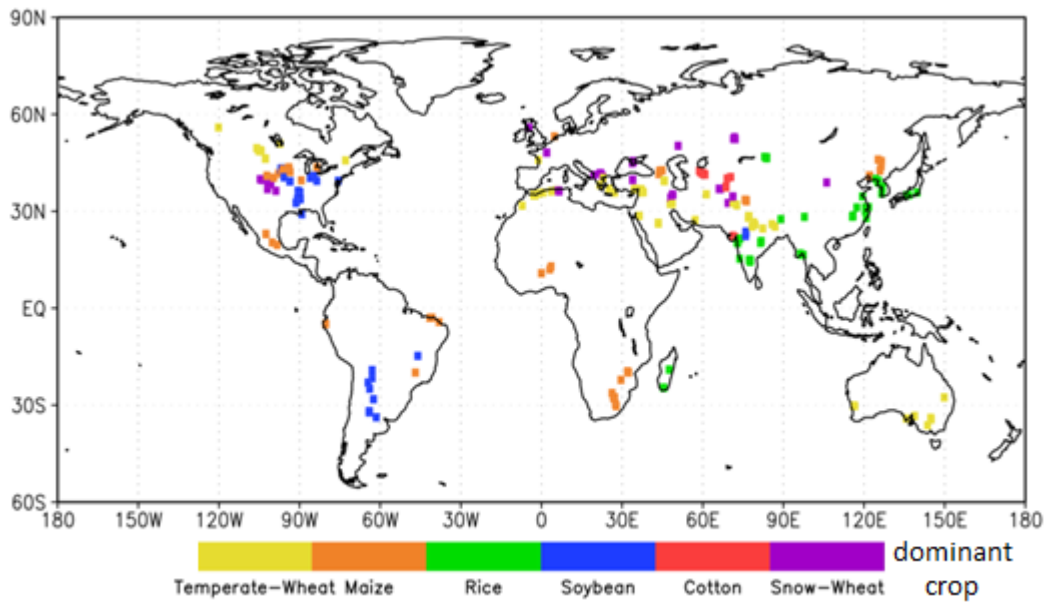
10



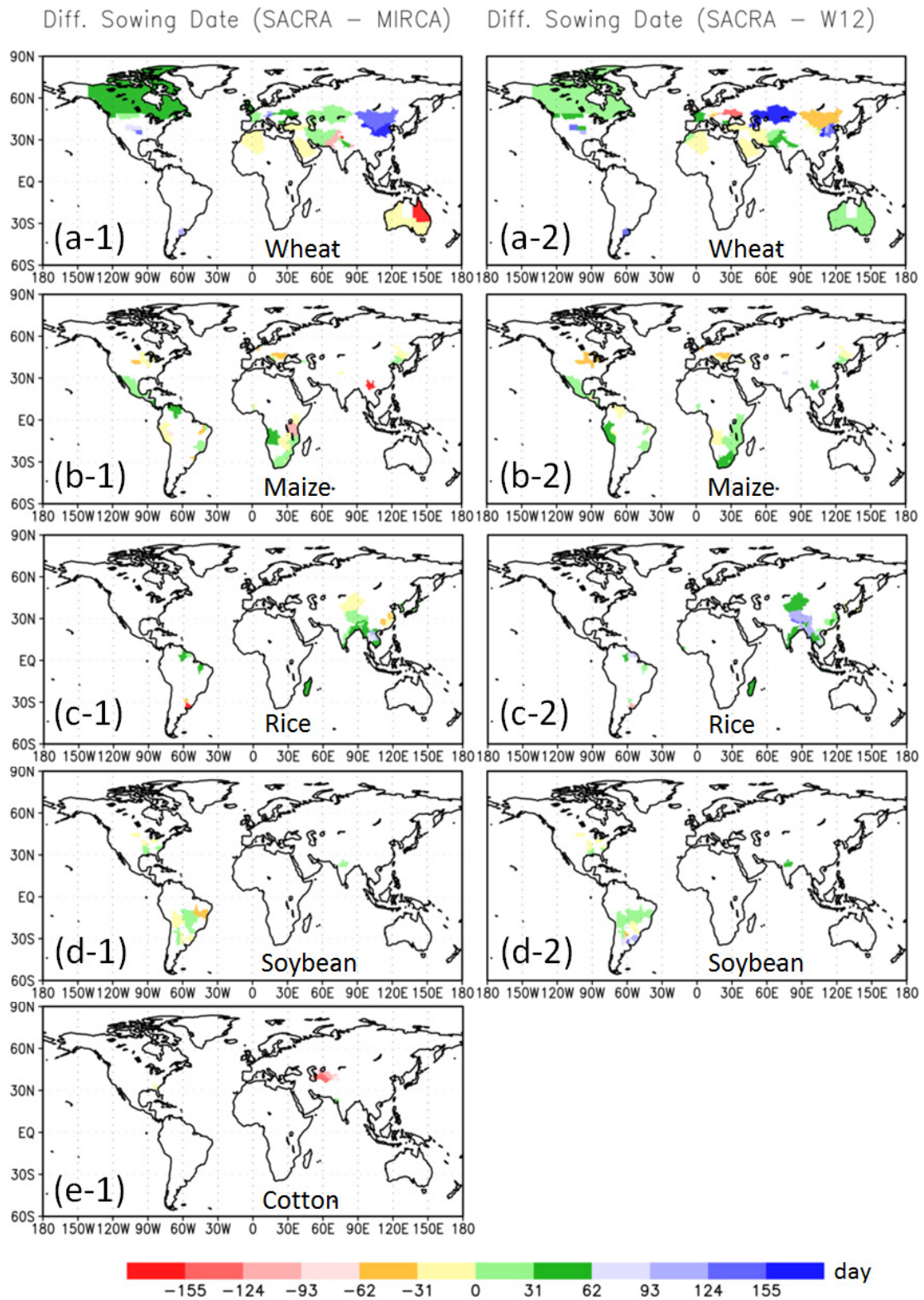


1

2 Fig. A1. Average error of sowing/harvesting dates (blue/orange lines; unit days) among  
 3 calibration grids for six crops (a: temperate-wheat, b: snow-wheat, c: maize, d: rice, e:  
 4 soybean, and f: cotton). Dots in the figures represent minimized errors and  
 5  $nNDVI_{sw}/nNDVI_{hv}$  (i.e., the calibrated two parameters in Table 4).  
 6

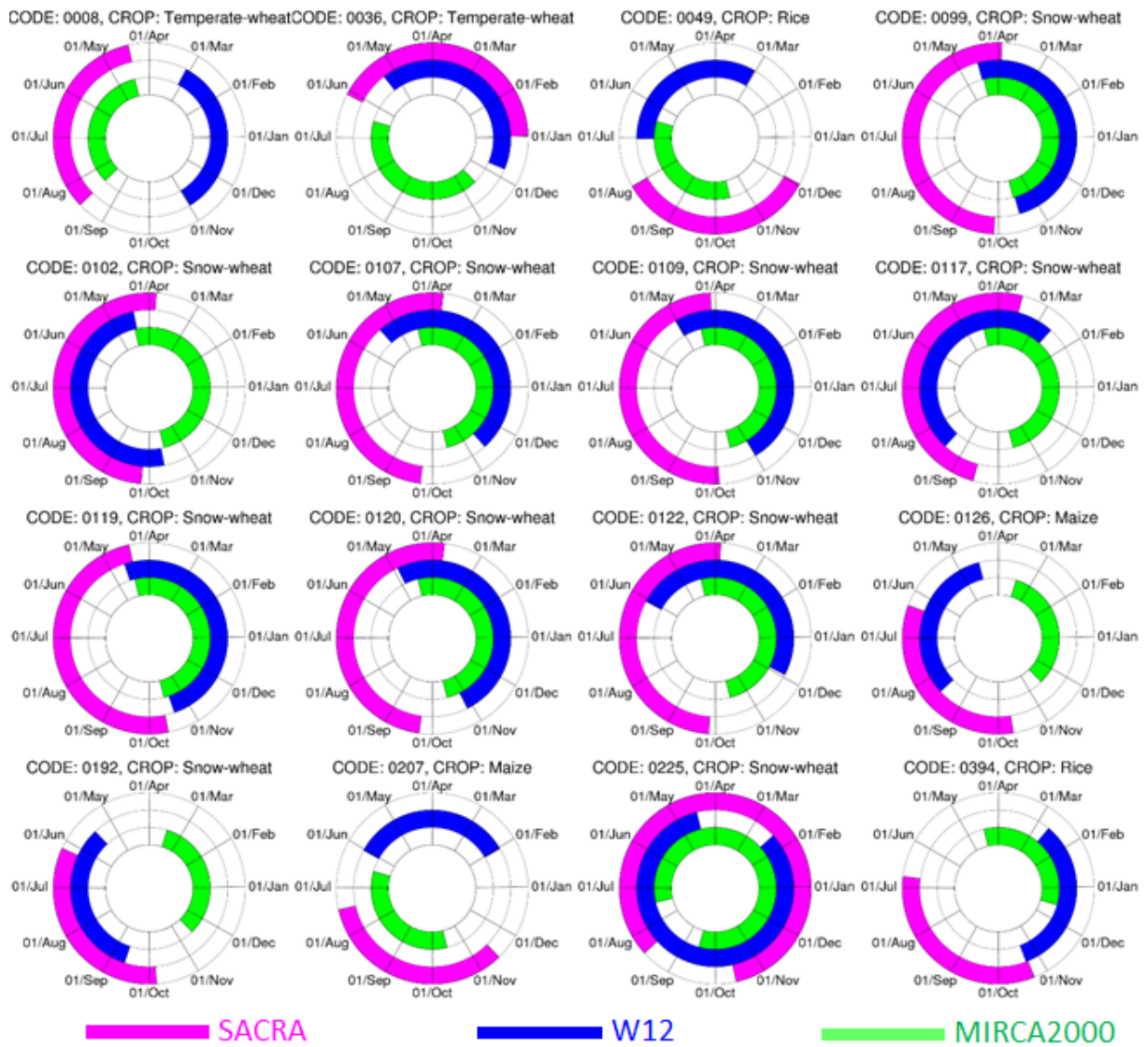


1  
 2 Fig. A2. Global distribution of calibration grids for the six crops. The calibration grids are  
 3 illustrated larger than the real grid size (5 arc-min) for emphasis.  
 4



1  
2  
3  
4  
5

Fig. A3. Same as Fig. 9 but for five specific crops (wheat, maize, rice, soybean, and cotton). The sowing date of cotton was not estimated by Waha et al. (2012). Only single cropping grids are used to compute the averaged sowing date for SACRA.



2 Fig. A4. Cultivation seasons (from sowing to harvesting dates) in 16 administrative units in  
 3 Table 5. Magenta, blue, and green denote SACRA, Waha et al. (2012) and MIRCA2000,  
 4 respectively. For Waha et al. (2012), we apply the cultivation period of MIRCA2000 for  
 5 purposes of illustration at each administrative unit. The beginning and end of the labels  
 6 represent averaged sowing and harvesting dates, respectively, over the administrative  
 7 unit. Only single cropping grids are used to compute the averaged sowing date for  
 8 SACRA.